Articles

Heteronuclear 2D NMR Studies of an Engineered Insulin Monomer: Assignment and Characterization of the Receptor-Binding Surface by Selective ^2H and ^{13}C Labeling with Application to Protein Design†

Michael A. Weiss,*,‡,§ Qing-Xin Hua,‡,∥ Claire S. Lynch,⊥ Bruce H. Frank,# and Steven E. Shoelson*,⊥

Department of Biological Chemistry and Molecular Pharmacology, Harvard Medical School, Boston, Massachusetts 02115, Department of Medicine, Massachusetts General Hospital, Boston, Massachusetts 02114, Joslin Diabetes Center and Departments of Medicine, Brigham and Women's Hospital and Harvard Medical School, Boston, Massachusetts 02215, and Lilly Research Laboratories, Eli Lilly & Company, Indianapolis, Indiana 46285

Received December 7, 1990; Revised Manuscript Received April 22, 1991

ABSTRACT: Insulin provides an important model for the application of genetic engineering to rational protein design and has been well characterized in the crystal state. However, self-association of insulin in solution has precluded complementary 2D NMR study under physiological conditions. We demonstrate here that such limitations may be circumvented by the use of a monomeric analogue that contains three amino acid substitutions on the protein surface (HisB10 → Asp, ProB28 → Lys, and LysB29 → Pro); this analogue (designated DKP-insulin) retains native receptor-binding potency. Comparative ^1H NMR studies of native human insulin and a series of three related analogues—(i) the singly substituted analogue [HisB10 → Asp], (ii) the doubly substituted analogue [ProB28 → Lys; LysB29 → Pro], and (iii) DKP-insulin—demonstrate progressive reduction in concentration-dependent line-broadening in accord with the results of analytical ultracentrifugation. Extensive nonlocal interactions are observed in the NOESY spectrum of DKP-insulin, indicating that this analogue adopts a compact and stably folded structure as a monomer in overall accord with crystal models. Site-specific ^2H and ^{13}C isotopic labels are introduced by semisynthesis as probes for the structure and dynamics of the receptor-binding surface. These studies confirm and extend under physiological conditions the results of a previous 2D NMR analysis of native insulin in 20% acetic acid [Hua, Q. X., & Weiss, M. A. (1991) *Biochemistry 30*, 5505–5515]. Implications for the role of protein flexibility in receptor recognition are discussed with application to the design of novel insulin analogues.

Insulin-like peptides represent an ancestral and highly conserved motif of protein folding and as a class provide an important model for the study of protein dynamics in macromolecular recognition. Insulin, the most highly characterized member of this class, is composed of two polypeptide chains, the A-chain (21 residues) and the B-chain (30 residues) linked by two disulfide bonds. Interest in structure–function relationships has recently been stimulated by the application of protein engineering to insulin as a target for rational drug design (Brange et al., 1988, 1990). In this paper we describe isotope-aided ^1H NMR[1] studies of a series of insulin analogues that exhibit altered self-association and pharmacokinetic properties. The long-term goal of these studies is to determine the structure and dynamics of an engineered insulin monomer under physiological conditions. By correlating structure with function, such studies may establish design rules for modified insulins as a model for targeted protein modification in molecular pharmacology.

Both the A- and B-chains contribute to the functional surface of insulin (Pullen et al., 1976; Baker et al., 1988), which has been extensively probed by comparative study of analogues and species variants (Figure 1A). Of particular interest is the C-terminal region of the B-chain (B23–B26). This region is highly conserved among vertebrate insulins (Dayhoff, 1972; Steiner et al., 1989) and appears to play a central role in insulin action (Pullen et al., 1976; Nakagawa & Tager, 1986, 1987; Mirmira & Tager, 1989). Surprisingly,

† This work was supported in part by an NIH grant to M.A.W. and an NSF grant to S.E.S. Peptide synthesis was supported by an NIH DERC grant to the Joslin Diabetes Center. Two of the authors (M.A.W. and S.E.S.) were also each supported by Research and Career Development Awards from the American Diabetes Association and grants from the Juvenile Diabetes Foundation International. M.A.W. is supported in part by the Pfizer Scholars Program for New Faculty and the American Cancer Society; S.E.S. is a Capps Scholars in Diabetes at Harvard Medical School.

* Address correspondence to either author at Harvard Medical School.
‡ Department of Biological Chemistry and Molecular Pharmacology, Harvard Medical School.
§ Massachusetts General Hospital.
∥ Permanent address: Institute of Biophysics, Academia Sinica, Beijing, China.
⊥ Joslin Diabetes Center and Departments of Medicine, Brigham and Women's Hospital and Harvard Medical School.
Eli Lilly & Co.

[1] Abbreviations: AspB10-insulin, human insulin containing the mutation HisB10 → Asp; CD, circular dichroism; DKP-insulin, insulin analogue containing three mutations (HisB10 → Asp; ProB28 → Lys; LysB29 → Pro); DOI, des-octapeptide insulin or insulin analogue lacking residues B23–B30; DPI, des-pentapeptide insulin or insulin analogue lacking residues B26–B30; DQF-COSY, double-quantum filtered correlated spectroscopy; HMQC, heteronuclear multiple-quantum correlation spectroscopy; HPLC, high-performance liquid chromatography; KP-insulin, insulin analogue containing two mutations (ProB28 → Lys and LysB29 → Pro); NMR, nuclear magnetic resonance; NOE, nuclear Overhauser enhancement; NOESY, 2D NOE spectroscopy; TOCSY, 2D total correlation spectroscopy by isotropic mixing.

0006-2960/91/0430-7373$02.50/0

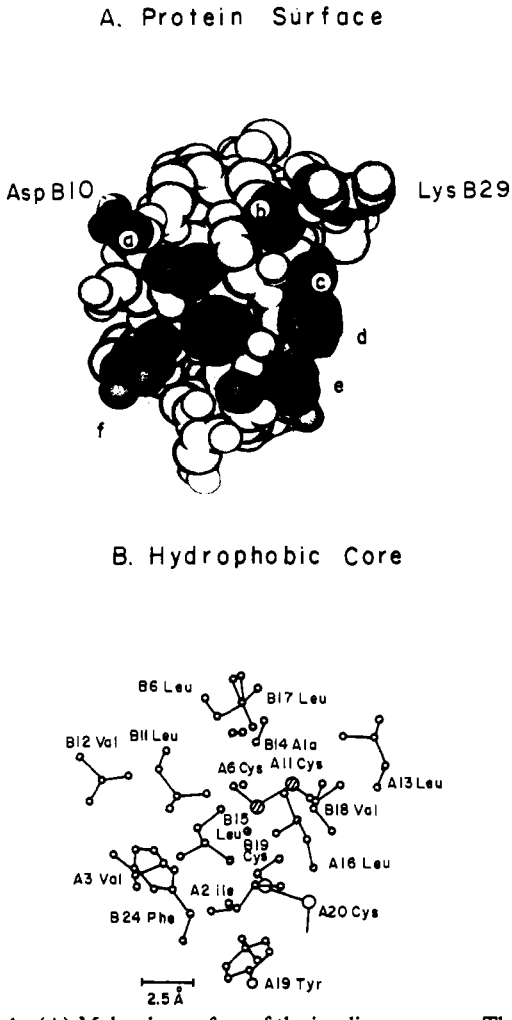

FIGURE 1: (A) Molecular surface of the insulin monomer. The three sites of mutation in DKP-insulin [HisB10 → Asp (labeled a), ProB28 (labeled c) → Lys, and LysB29 (labeled b) → Pro] are shown in black, and a subset of putative receptor-binding residues (B12, B16 (labeled f), B23 (e), B25 (d), and A21) are shown in gray. This figure was adapted from Brange et al. (1990) with permission of the authors. (B) Hydrophobic core of the insulin monomer in the 2-Zn crystal (molecule 2) as viewed down the *c* axis (Baker et al., 1988).

the receptor-binding properties of certain naturally occurring and synthetic C-terminal analogues (Tager et al., 1979; Shoelson et al., 1983a,b; Nakagawa & Tager, 1986, 1987; Mirmira & Tager, 1989) are difficult to rationalize from the structure of insulin in the crystal state (Adams et al., 1969; Blundell et al., 1971; Peking Insulin Structure Group, 1971; Dodson et al., 1983; Smith et al., 1984; Baker et al., 1988). These observations suggest that nonlocal displacements of residues B23–B30 might be required in the hormone–receptor complex (Dodson et al., 1979, 1984; Baker et al., 1988; Mirmira & Tager, 1989).

The structure and dynamics of the receptor-binding surface of insulin have not been well characterized in aqueous solution. Detailed NMR study has been limited in the past by insulin self-association (formation of dimers, tetramers, hexamers, and higher order oligomers; Jeffrey & Coates, 1966a,b; Goldman & Carpenter, 1976), which occurs in native insulin at the concentrations required for acquisition of 2D NMR data (Kowalsky, 1962; Bradbury & Wilairat, 1967; Paselk & Levy, 1974; Bradbury & Brown, 1977; Williamson & Williams, 1979; Bradbury et al., 1981). High-resolution spectra have been analyzed under strongly basic conditions (Bradbury & Ramesh, 1985; Hua et al., 1989) or under acidic conditions in mixed-solvent systems (Williamson et al., 1981; Cheshnovsky et al., 1983; Weiss et al., 1989). Sequential assignment of native human insulin has been described in 35% acetonitrile at pH 3.6 (Kline & Justice, 1990) and of a des-pentapeptide insulin (DPI; lacking residues B26–B30) at pH 1.8 (Boelens et al., 1990) and in 20% acetic acid (Hua & Weiss, 1990). In an important advance, Dunn and colleagues have recently demonstrated that SerB9 → Asp insulin, an analogue with reduced self-association, can be used to obtain high-resolution one-dimensional ^{1}H NMR spectra at neutral to basic pH (Roy et al., 1990). The sequential assignment of a dimeric form of this analogue has also been described at pH 1.8 (Kristensen et al., 1991).

In this paper we extend this approach to a series of insulin analogues containing one, two, or three amino acid substitutions on the surface of the protein (Figure 1A). One substitution (HisB10 → Asp) destabilizes the hexamer contact and was originally described in association with a clinical syndrome of hyperproinsulinemia and diabetes mellitus in man (Grappuso et al., 1984; Chan et al., 1987). Two substitutions (ProB28 → Lys and LysB29 → Pro) destabilize the dimer interface and were originally designed and characterized at Eli Lilly & Co. Each of these analogues exhibits native or slightly increased affinity for the insulin receptor.

Our results are presented in three parts. In part I the rationale underlying the design of DKP-insulin is presented. ^{1}H NMR spectra of native human insulin and the three related analogues—(i) the singly substituted analogue [HisB10 → Asp], (ii) the doubly substituted analogue [ProB28 → Lys; LysB29 → Pro], and (iii) the triply substituted analogue [HisB10 → Asp; ProB28 → Lys; LysB29 → Pro], designated DKP-insulin—are shown under physiological conditions to exhibit progressive reduction in concentration-dependent line-broadening in accord with the results of analytical ultracentrifugation. Although DKP-insulin exhibits high-quality 2D NMR spectra in D_2O, base-catalyzed amide proton exchange in H_2O precludes sequential assignment in key regions of the protein. As an alternative assignment method, site-specific ^{2}H and ^{13}C labels are incorporated by trypsin-catalyzed semisynthesis at positions B23–B26 (Figure 2); these labels are shown in part II to provide rigorous ^{1}H and ^{13}C resonance assignments. Long-range NOEs within and between the A- and B-chains are analyzed in part III. These NOE patterns are shown to reflect the solution structure and dynamics of the C-terminal region of the B-chain and its relationship to the underlying hydrophobic core. Presumptive assignment of these NOEs is obtained by comparison with sequential assignments reported under acidic conditions or in mixed acid/organic solvent systems (Kline & Justice, 1990; Boelens et al., 1990; Hua & Weiss, 1990, 1991); further analysis is presented in reference to crystal structures of native and modified insulins (Blundell et al., 1971; Peking Insulin Structure Group, 1971; Dodson et al., 1983; Bi et al., 1984; Baker et al., 1988). Implications of this work for the mechanism of insulin action and the design of novel insulin analogues are considered in the Discussion section.

Materials and Methods

Biosynthetic native human insulin was provided as zinc crystals by Eli Lilly & Company (Indianapolis, IN). Zinc was removed by gel filtration (G-25 Sephadex) in 1% acetic acid. The solution was lyophilized and redissolved in NMR buffer (below). Insulin concentrations were determined by UV absorbance at 278 nm, assuming that a 1 mg/mL solution has an absorbance of 1.05/cm (Frank & Veros, 1968). Unlabeled mutant insulins containing the substitutions [HisB10 → Asp], [ProB28 → Lys; LysB29 → Pro], and [HisB10 → Asp;

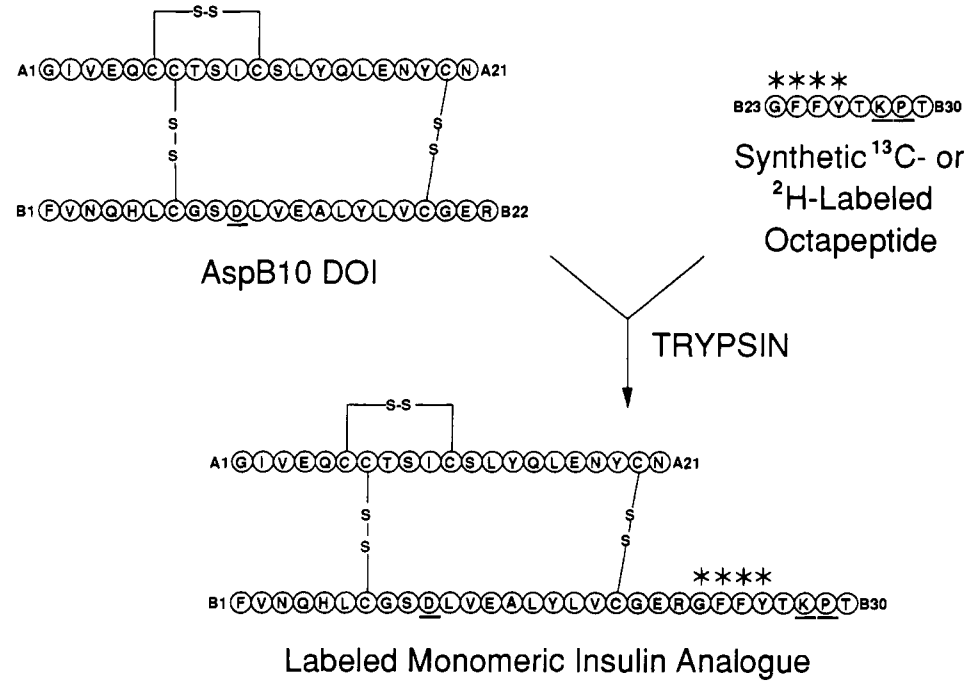

FIGURE 2: Primary structure of DKP-insulin (one-letter code) and scheme for semisynthesis of ^{13}C- and ^{2}H-labeled monomeric insulin analogues. [HisB10 → Asp]des-octapeptide insulin (AspB10-DOI) and a synthetic octapeptide (Gly-Phe-Phe-Tyr-Thr-*Lys-Pro*-Thr) are dissolved in an aqueous organic cosolvent and allowed to react in the presence of trypsin (see text; Materials and Methods). Asterisks represent positions within the octapeptides and insulin analogues that were substituted with residues enriched in ^{13}C and ^{2}H. Italicized residues differ from native human insulin (HisB10 → Asp; ProB28 → Lys; LysB29 → Pro); these changes markedly reduce the self-association of the analogue without loss of bioactivity (Table I).

ProB28 → Lys; LysB29 → Pro] (designated AspB10-insulin, KP-insulin, and DKP-insulin, respectively) were kindly provided by Eli Lilly & Co. and used without further purification.

^{2}H- and ^{13}C-Labeled Peptide Synthesis and Purification. t-Boc-L-[*ring*-$^{13}C_6$]phenylalanine and t-BOC-L-[*ring*-$^{2}H_5$]-phenylalanine were prepared by treatment of L-[*ring*-$^{13}C_6$]-phenylalanine and L-[*ring*-$^{2}H_5$]phenylalanine (Cambridge Isotope Laboratories, Woburn, MA), respectively, with 2-(((t-butoxycarbonyl)oxy)imino)-2-phenylacetonitrile (BOC-ON, Aldrich) as described (Steward & Young, 1984). t-BOC-L-[*ring*-$^{2}H_4$]tyrosine(0-Bzl) and t-BOC-[1,2-$^{13}C_2$]glycine were supplied by Cambridge Isotope Laboratories, Inc. Additional unlabeled protected amino acids and reagents were purchased from Applied Biosystems; solid-phase syntheses were performed on an Applied Biosystems Model 430A synthesizer. All synthetic peptides have the general sequence NH-Gly-Phe-Phe-Tyr-Thr-*Lys-Pro*-Thr-OH, which corresponds to insulin residues B23–B30 with inversion of ProB28 and LysB29 (italics). Peptide syntheses were initiated using 0.5 mmol of t-BOC-Thr(Bzl)-PAM resin (0.62 mmol/g) with standard protocols for DCC-mediated preformed symmetrical anhydride coupling. After synthesis of the first four residues (t-BOC-Thr-Lys-Pro-Thr-PAM), the resin-bound peptide was divided into five equal aliquots (0.1 mmol/aliquot), and syntheses were continued on this smaller scale. Protected ^{13}C- and ^{2}H-labeled amino acids derivatives (see above) were incorporated as preformed HOBt esters using 2.0-h coupling times to minimize waste of label. The final peptide products were cleaved from the resin with use of an anhydrous mixture of 20% trimethylsilyl trifluoromethanesulfonate, 12% thioanisole, 6% ethanedithiol, and 2% *m*-cresol in trifluoroacetic acid (Yajima et al., 1988), filtered, precipitated with ice-cold diethyl ether, desalted on a column (Bio-Gel P2; 2.6 × 100 cm) equilibrated in 3 M acetic acid, and lyophilized. Isolated ^{2}H- and ^{13}C-labeled peptides were purified by reversed-phase HPLC on an RP-318 column (Bio-Rad; 21.5 × 250 mm); after an initial 3.0-min isocratic elution at 15% acetonitrile in 0.05 aqueous trifluoroacetic acid (20 mL/min), the acetonitrile composition was increased linearly at a rate of 1.0% every 5.0 min. In each case a single predominant peak was resolved at an elution time similar to that of the unlabeled octapeptide.

Table I: Relative Receptor-Binding Affinities and Oligomeric States of Insulin Analogues

analogue	potency[a]	oligomeric state[b]
native human insulin	1	4
[HisB10 → Asp]	2	2
[ProB28 → Lys; LysB29 → Pro]	1	1.8
[HisB10 → Asp; ProB28 → Lys; LysB29 → Pro]	2	1

[a] Bioactivity relative to ^{125}I-labeled human insulin was measured with use of an isolated receptor binding assay as described in the Materials and Methods section. [b] Oligomeric state (apparent MW/monomer MW) was measured at a protein concentration of 0.6 mM by analytical ultracentrifugation in a buffer consisting of 200 mM NaCl and 50 mM sodium phosphate (pH 7).

Preparation of ^{2}H and ^{13}C-Labeled Monomeric Analogues. Des-octapeptide HisB10 → Asp human insulin (AspB10-DOI), kindly provided by R. E. Chance (Eli Lilly & Co., Indianapolis, IN), was prepared by treatment of biosynthetic HisB10 → Asp proinsulin with TPCK–trypsin (Bromer & Chance, 1967). Trypsin-catalyzed semisyntheses were conducted with AspB10-DOI and labeled octapeptides in a modification of a previously described method (Shoelson et al., 1983b; Kubiak & Cowburn, 1986; Nakagawa & Tager, 1986; Shoelson et al., 1991). Analogues were characterized by HPLC, amino acid composition, and fast atom bombardment mass spectrometry (FAB-MS; Yale University).

Insulin Receptor-Binding Assays. As a functional control, the receptor-binding activities of proteins used for NMR study were independently evaluated and compared to values previously reported (Table I). Human insulin receptor was isolated from CHO cells that were stably transfected with a human

cDNA construct (Ebina et al., 1985). The cells, expressing approximately 10^6 receptors/cell, were solubilized at 4 °C in 50 mM Hepes (pH 7.4)/1% Triton X-100/0.1 mg/mL aprotinin/2 mM PMSF in a final volume of 50 mL/mL of packed cells. Following centrifugation to remove insoluble debris, the extract was passed over a column (10 mL) of wheat germ agglutinin agarose (WGA–agarose, Vector); after washing of the column, adsorbed glycoproteins were eluted with 0.3 M *N*-acetylglucosamine in 50 mM Hepes (pH 7.4)/0.1% Triton X-100. Aliquots of WGA-purified receptor, A14-[^{125}I]monoiodoinsulin, and varying amounts of the insulin analogue were incubated together in 200 μL of 50 mM Hepes (pH 7.4)/0.1% Triton X-100 at 4 °C for 16 h. Insulin–receptor complexes were precipitated in the presence of 0.1% bovine γ-globulin with 12.5% poly(ethylene glycol) (final concentration).

Oligomeric State. Equilibrium ultracentrifuge studies were conducted by using the photoelectric scanning optical system as described (Pekar & Frank, 1972). The information on the scanner-chart recording was processed with the internal calibration factors of the scanner. The resulting weight-average molecular weight data were fitted to a model involving initial dimerization followed by isodesmic self-association of dimers up to and including a 14-mer (Jeffrey et al., 1976) to yield the self-association constants for each analogue.

NMR. Spectra were recorded at 500 MHz at Harvard Medical School and the University of Wisconsin High-Field NMR Resource. Two-dimensional experiments were performed by the pure-phase method of States et al. (1982). A total of 2048 points were sampled in t_2; 400 t_1 values were obtained, and the data matrix was zero-filled to 2K × 2K. TOCSY and NOESY spectra were processed by use of shifted sine-bell window functions with exponential apodization in both dimensions; DQF-COSY spectra were processed similarly, with the addition of a squared sine-bell function. HMQC experiments were performed as described by Davis and Bax (1986). Spectra recorded at the first t_1 value provide one-dimensional isotope-edited ^{1}H NMR spectra (Figure 8). ^{13}C decoupling was accomplished during ^{1}H acquisition using the WALTZ-16 scheme. Ring-current effects (Johnson & Bovey, 1958) were calculated on the basis of crystal structures of native porcine insulin as described (Hoch et al., 1982; Weiss & Hoch, 1987). Predicted NOEs were back-calculated from crystal structures using the matrix-relaxation method implemented in the program XPLOR (A. T. Brunger, Yale University).

NMR Buffers. Samples were prepared under two conditions. (i) Low ionic strength buffer: the protein was dissolved in distilled H_2O (or D_2O), and the pH (or pD) was adjusted to 8.0 (direct meter reading) with small aliquots of dilute HCl (or DCl) as described by Roy et al. (1990). (ii) Phosphate-buffered saline: the protein was dissolved in 140 mM NaCl/10 mM sodium phosphate (pH or pD adjusted in the range 6.5–8.0). The spectrum of DKP-insulin is essentially identical under the two sets of conditions.

RESULTS

(I) Overview of Protein Design

Analysis of the insulin surfaces involved in crystallographic packing interactions has led to the design of mutant insulins with altered self-association properties (Brange et al., 1988). Because distinct interactions are involved in dimer and hexamer packing, these contacts may be independently modified by protein engineering. In this section DKP-insulin is described as a model system for two-dimensional ^{1}H NMR studies of the insulin monomer. The sequence of human insulin and sites of modification (residues B10, B28, and B29) are shown in Figure 2. The relative receptor-binding affinities and oligomeric states of these modified insulins are given in Table I. The rationale underlying design of DKP-insulin was developed at the Lilly Research Laboratories and is reviewed in the Discussion section.

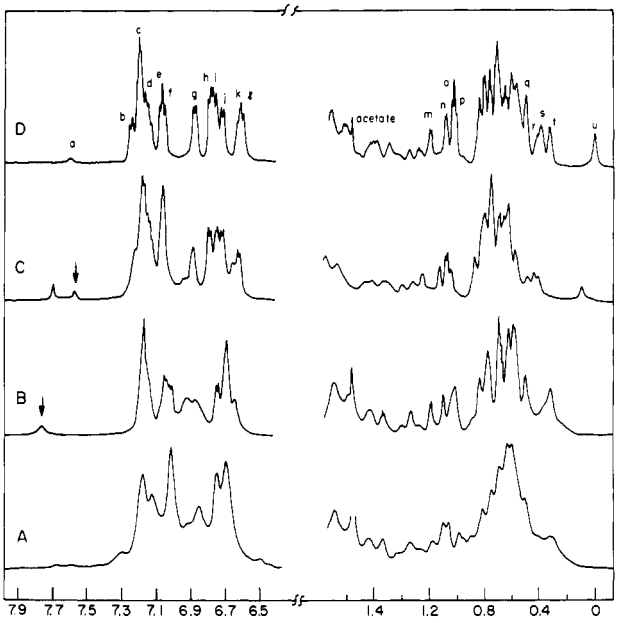

FIGURE 3: Aromatic and methyl regions of 500-MHz ^{1}H NMR spectra in D_2O at pD 8 and 37 °C of (A) native human insulin, (B) [HisB10 → Asp]insulin, (C) [ProB28 → Lys; LysB29 → Pro]insulin, and (D) DKP-insulin. Assignments of resonances a–u in panel D are given in Tables II and IV. Arrows in panels B and C indicate C_2H resonance of HisB5, whose chemical shift is sensitive to dimerization; the HisB5-C_2H resonance in DKP-insulin is labeled a in panel D. Spectra were apodized with 2-Hz exponential multiplication before Fourier transformation. The spectra are the sum of 128 scans. The protein concentration in panels A and B was 1 mM; the protein concentration in panels C and D was 0.75 mM. The proteins were lyophilized from 1% acetic acid; a residual acetate methyl resonance (1.48 ppm) is observed in panels A, B, and D. Resonances a–u are assigned as follows: (a) HisB5-C_2H, (b) TyrA19-ortho, (c) TyrB16-ortho, PheB1-meta/para, and PheB25-meta/para, (d) PheB25-ortho, (e) PheB1-ortho, (f) TyrA14-ortho, (g) PheB24-para and TyrB26-ortho, (h) TyrA14-meta and PheB24-meta, (i) TyrB16-meta, (j) TyrA19-meta, (k) PheB24-ortho, (l) TurB26-meta, (m) AlaB14-βCH_3, (n–p) three Thr-βCH_3 (q) IleA10-$\gamma' CH_3$ and LeuB16-δCH_3, (r) IleA2-δCH_3, (s) LeuB15-$\delta_1 CH_3$, (t)IleA10-$H_{\gamma 1}$ and -δCH_3 (u) LeuB15-$H_{\beta 2}$ and -$\delta_1 CH_3$. No stereospecific assignments are obtained.

(*i*) *Native Insulin.* At millimolar concentrations human insulin exists as a complex distribution of monomers, dimers, tetramers, hexamers, and higher order oligomers (Jeffrey & Coates, 1966a,b; Goldman & Carpenter, 1974). These coupled equilibria result in broadening of ^{1}H NMR resonances by intermediate-exchange mechanisms and by hindered rotation of higher molecular weight species. These effects are illustrated in panel A of Figure 3 (1D ^{1}H NMR spectrum) and panel A of Figure 4 (2D ^{1}H NMR DQF-COSY spectrum); few cross-peaks are observed in the latter spectrum due to antiphase cancellation of the two-dimensional multiplets (see figure caption). Significant concentration-dependent changes in resonance line width and chemical shifts are observed under these conditions over a 20 μM to 2 mM range of protein concentrations (Roy et al., 1990).

(*ii*) *[HisB10 → Asp]Human Insulin.* The effects of a mutation in the hexamer interface (HisB10 → Asp) are shown in panel B of Figure 3. This analogue is predominantly dimeric at the concentration and conditions used (Table I) and exhibits

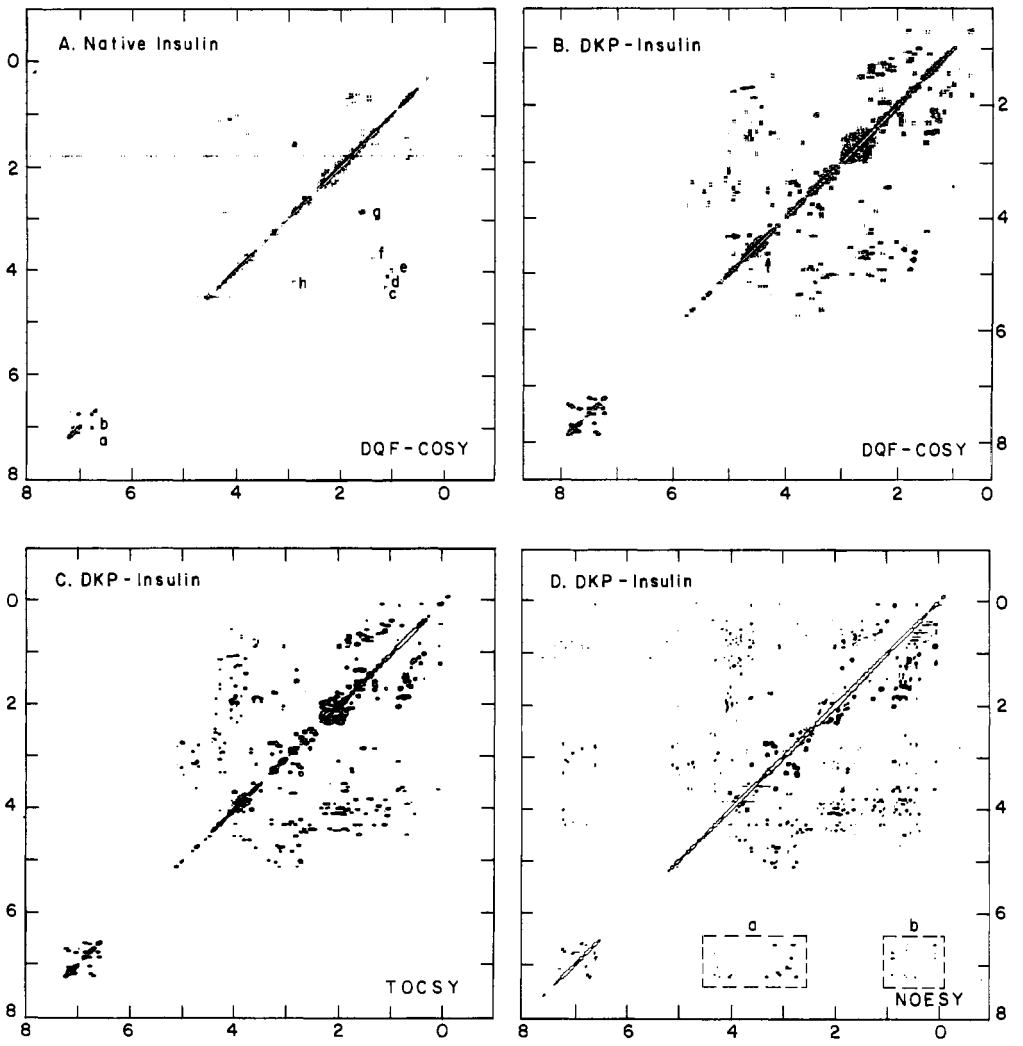

FIGURE 4: (A) DQF-COSY spectrum of native human insulin demonstrating extensive attenuation of spin systems by antiphase cancellation. In contrast, DQF-COSY and TOCSY spectra of DKP-insulin (panels B and C, respectively) exhibit an expected number of amino acid spin systems. These include one alanine (B14), two isoleucines (A2 and A10), three threonines (A8, B27 and B30), six leucines (A13, A16, B6, B11, B15, and B17), and four valines (A3, B2, B12, and B18); there are no methionine residues. (D) NOESY spectrum of DKP-insulin exhibiting numerous interresidue effects, mixing time of 200 ms. Cross-peaks observed in panel A (native insulin) represent spin systems whose line widths are not disproportionately broadened by intermediate exchange among oligomeric species; these include (a) TyrA19-ortho/meta, (b) TyrA14-ortho/meta, (c–e) three Thr-H_{β}–CH_3 (f) AlaB14-H_{α}–βCH_3, (g) LysB29-H_{δ}–H_{ϵ}, and (h) unassigned. The arrow in panel B indicates the $H_{\alpha 1}$–$H_{\alpha 2}$ cross-peak of GlyB23 (see also Figure 7). In panel D aromatic-$H_{\alpha/\beta}$ and aromatic-methyl regions of the NOESY spectrum are indicated (boxes a and b, respectively); these regions are shown in expanded form in Figures 9 and 10. The upfield portion (0.2 ppm) of the TOCSY spectrum (panel C) is shown in expanded form in Figure 11. Spectra were recorded at 37 °C in D_2O solution (pD 8.0, direct meter reading).

a 2-fold increase in receptor-binding activity (Schwartz et al., 1987; Brange et al., 1988; Table I). A general reduction in line widths is observed (relative to the spectrum of native insulin) due to the absence of tetrameric, hexameric, and higher order oligomers. Perturbations in chemical shift are also seen, which presumably arise from changes in promoter conformation with self-association. The 2D NMR spectrum of the AspB10-insulin dimer will be described in detail elsewhere (manuscript in preparation); an NMR study of the related AspB9 dimer has recently been published (Kristensen et al., 1991).

(iii) [ProB28 → Lys; LysB28 → Pro]Human Insulin. The effects of a complementary modification of the dimer interface ([ProB28 → Lys; LysB28 → Pro]) are shown in panel C of Figure 3. Near-UV CD studies demonstrate that this modification reduces specific dimerization by at least a factor of 10^3 (B.H.F., unpublished results); however, residual self-association is observed at high protein concentrations by equilibrium ultracentrifugation, presumably via the hexamer interface (Table I). The ^1H NMR spectrum also demonstrates marked reduction in line widths relative to native insulin; further reduction in resonance line width is observed at lower protein concentrations (data not shown), consistent with the ultracentrifugation studies. Chemical shift differences are observed relative to native insulin oligomers and the AspB10 dimeric analogue, similar to those previously described in a SerB9 → Asp analogue (Roy et al., 1990). Such differences may reflect either changes in protomer conformation upon dimer and hexamer formation or ring-current effects in the subunit interfaces. The receptor-binding affinity of KP-insulin is similar to that of native human insulin (Table I).

(iv) DKP-Insulin as an NMR Model System. The ^1H NMR spectrum of [HisB10 → Asp; ProB28 → Lys; LysB28 → Pro]insulin (DKP-insulin) is shown in panel D of Figure 3. The line widths are appropriate for a protein of monomer molecular mass 6 kDa, and no changes in line width or chemical shift are observed in the concentration range 15 μM to 2.5 mM (data not shown). Partial assignments of resonances a–u are presented below (parts II and III of Results) and summarized in Tables II and IV. Analytical ultracen-

Table II: Selected ^{1}H NMR Assignments of DKP-Insulin at pD 8.0 and 37 °C (parts per million relative to H_2O at 4.7 ppm)

spin system	$C_\alpha H$	$C_\beta H$	other		
		(A) Unique Spin Systems			
AlaB14	3.95	1.24			
HisB5	4.30	2.96, 3.30	C_2H 7.54	C_4H 6.72	
			H_γ	H_δ	H_ϵ
ArgB22	4.06	2.06, 1.96	1.76, 1.76	3.22, 3.28	
LysB28	4.31	1.70, 1.63	1.34, 1.34	1.53, 1.53	2.84, 2.84
ProB29	4.37	2.19, 1.89	1.87, 1.87	3.52, 3.66	
		(B) Isotope-Based Assignments			
GlyB23	(3.67, 4.00)		ortho	meta	para
PheB1[a,b]	4.30	2.84, 2.67	7.06	7.17	7.10
PheB24	5.13	3.15, 2.80	6.62	6.77	6.86
PheB25	4.74	3.10, 3.10	7.11	7.18	7.13
TyrB26	4.53	2.84, 2.84	6.86	6.66	
		(C) NOE-Based Aromatic Assignments[c]			
TyrA14	4.25	2.92, 2.92	7.04	6.78	
TyrA19	4.21	3.31, 2.74	7.23	6.70	
TyrB16	4.31	3.06, 3.06	7.18	6.74	

[a] The assignments of PheB1 are by elimination. [b] The respective ortho and meta ring resonances of the phenylalanine and tyrosine rings are in fast exchange on the ^{1}H NMR time scale. [c] Presumptive assignments are obtained by analogy to sequential assignments in acid/organic cosolvents (Hua & Weiss, 1991) and in reference to crystal structures.

trifuge studies demonstrate that, unlike KP-insulin, DKP-insulin is truly monomeric in this range of protein concentrations; the receptor-binding affinity of DKP-insulin is similar to that of AspB10-insulin, i.e., about 2-fold greater than that of native human insulin (Table I).

2D NMR and Assignment of Unique Spin Systems. DKP-insulin exhibits a dramatic improvement in the quality of the 2D NMR spectra (Figure 4). DQF-COSY (panel B) and TOCSY (panel C) spectra contain the expected number of amino acid spin systems, and the NOESY spectrum (panel D) reveals significant interresidue contacts. Interresidue NOEs involving aromatic protons (spectral regions labeled a and b in panel D) are described below (part III of Results). These spectra demonstrate that DKP-insulin adopts a well-defined folded structure in solution. Nevertheless, the overall number of interresidue NOEs is less than would be predicted by a multispin analysis of crystal models. The absence or attenuation of interresidue NOEs is likely to reflect a dynamic process and will be analyzed in detail elsewhere (manuscript in preparation).

DKP-insulin contains one each of the following residues: AlaB14, ArgB22, LysB28, and ProB29. Assignment of their distinctive spin systems (Wuthrich, 1986) is given in Table II. LysB28 and ProB29 are sites of mutation in DKP-insulin. Observation of B28-H_α/B29-H_δ NOEs indicates that the X–proline peptide bond is trans; no evidence is observed for cis–trans isomerization of proline. Interestingly, the two δ protons of ArgB22 exhibit inequivalent chemical shifts (Table II), suggesting that the orientation of the side chain is nonrandom. We speculate that this charged side chain participates in a salt bridge on the surface of the protein. Such inequivalence is not observed in 20% acetic acid, under which conditions partner carboxylate groups would be expected to be protonated.

Assignment of AspB10. 2D NMR spectra of the doubly substituted analogue KP-insulin at protein concentrations less than 1 mM are very similar to those of DKP-insulin, indicating that in this context the substitution HisB10 → Asp is structurally conservative (data not shown). This is a significant result, in that AspB10 is associated with hyperproinsulinemia in man (Grappuso et al., 1984; Chan et al., 1987), apparently as a result of intracellular missorting of the mutant proinsulin (Carrol et al., 1988; Gross et al., 1989). Comparison of the DQF-COSY and TOCSY spectra of the doubly substituted analogue (containing HisB10; panel A of Figure 5) and the triply substituted analogue (containing AspB10; panels B and C) permits assignment of their respective B10 spin systems. In DKP-insulin no significant interresidue NOEs are observed to AspB10, suggesting that it projects from the surface of the protein as shown in Figure 1A. The apparent absence of structural "cross-talk" between the B10 site and residues B23–B26 (assigned in part III; below) is consistent with observations by Katsoyannis and colleagues that modifications at these two sites exhibit additive effects on the potency of insulin analogues (Schwartz et al., 1989).

pH Dependence and Amide-Exchange Rates. Well-resolved ^{1}H NMR spectra of DKP-insulin may be obtained in the pH range 6–8. Below pH 6 (i.e., near the isoelectric point of the protein) the solution becomes opalescent with attendant broadening of NMR resonances. This phenomenon reflects a reversible polymerization and is also observed with native human insulin. The one-dimensional spectrum of the amide and aromatic resonances of DKP insulin in 90% H_2O/10% D_2O solution (pH 6.8) exhibits only a portion of the resonance amplitude expected for 50 (non-proline) residues, presumably due to rapid solvent exchange (Figure S1, supplementary material). An additional (non-solvent) exchange mechanism is suggested by the large variation observed in resonance line widths; this variation may reflect millisecond motions in the protein as previously described under acidic conditions in mixed organic solvent systems (Weiss et al., 1989, 1990; Kline & Justice, 1990). DKP-insulin also exhibits extensive variations in amide line widths as a monomer at pH 1.8 (data not shown). No slowly exchanging amide resonances are observed in solutions freshly prepared in D_2O (pH 6.8); the pattern of slowly exchanging amide resonances in 20% deuterated acetic acid is similar to that of native insulin (Hua & Weiss, 1991).

The limited pH range available for 2D NMR study above the isoelectric point (pH > 6) restricts the application of sequential assignment methods, since such strategies employ successive relationships among H_N and H_α "fingerprint" protons (Wuthrich et al., 1983; Wuthrich, 1989). The two-dimensional fingerprint is incomplete (data not shown); partial sequential assignment is possible, however, and will be described in detail elsewhere (manuscript in preparation). In the present study, alternative assignment methods are used on the basis of specific isotopic labeling. Such labeling enables residues B23–B26 in the putative receptor-binding surface to

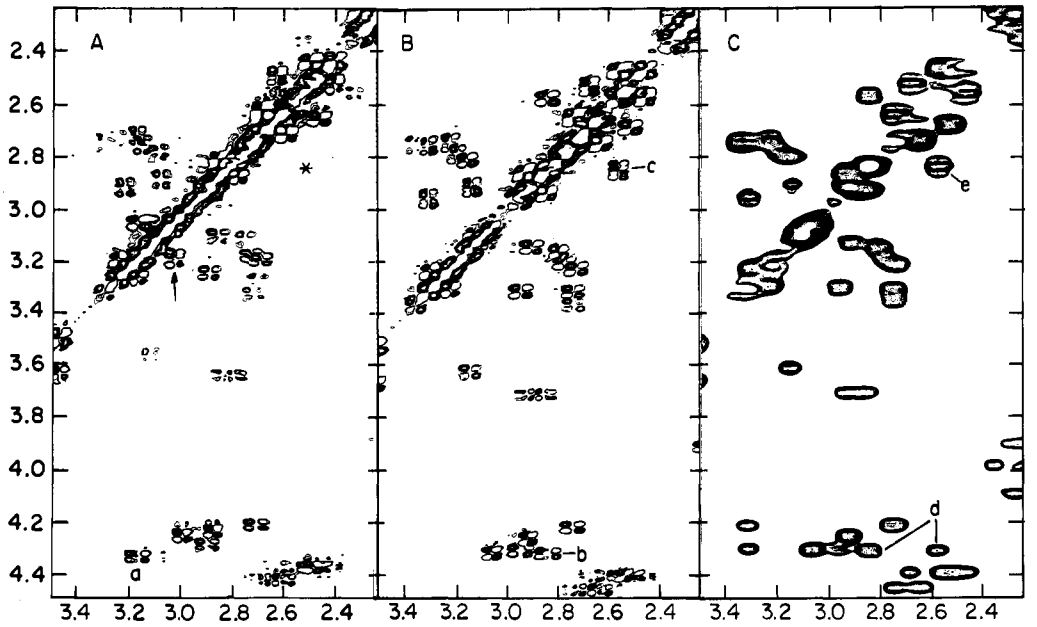

FIGURE 5: Assignment of ^{1}H NMR resonances of diabetes-associated side-chain AspB10 accomplished by comparison of spectra of doubly and triply substituted analogues: (A) region of DQF-COSY spectrum of analogue [ProB28 → Lys; LysB29 → Pro] showing HisB10 AMX spin system, (B) corresponding region of the DQF-COSY spectrum, and (C) TOCSY spectrum of DKP-insulin showing absence of HisB10 AMX spin system and new AMX system. The latter is presumptively assigned to AspB10. In each case the protein concentration was 0.75 mM at pD 8 (direct meter reading) and 37 °C; the TOCSY mixing time was 55 ms. In panel A the $\alpha\beta_1$ (labeled a) and β_{1-2} (arrow) cross-peaks of HisB10 are marked; the asterisk indicates the position of the AspB10 β_1–β_2 cross-peak, which is absent in this analogue. In panel B the corresponding α–β_1 (labeled b) and β_1–β_2 (c) cross-peaks of AspB10 are marked; in panel C the AspB10 α–β_1 and α–β_2 cross-peaks are labeled d and the β_1–β_2 cross-peak is labeled e.

Table III: ^{13}C Assignments (in parts per million)[a] of Labeled Residues B23–B26

residue	atom and assignment
GlyB23	C_α 43.0
PheB24[b]	C_δ 131.15, C_ϵ 129.4, C_ϵ 128.3
PheB25[b]	C_δ 130.75, C_ϵ 129.8, C_ϵ 128.2
TyrB26[b]	C_δ 131.20, C_ϵ 116.6

[a] Chemical shifts are measured relative to dioxane, assumed to be at 67.8 ppm. [b] The respective ortho (δ1 and δ2) and meta (ϵ1 and ϵ2) ^{13}C ring resonances of B24–B26 are equivalent, reflecting fast exchange on the ^{13}C NMR time scale; the attached proton resonances are also in fast exchange on the ^{1}H NMR time scale (Table II).

be identified (part II) and their local environments to be analyzed (part III).

(II) Assignment of ^{1}H and ^{13}C NMR Resonances

In this section NMR studies are described of DKP-insulin analogues containing isotopic labels at positions B23–B26. ^{1}H and ^{13}C assignments so obtained are given in Tables II and III, respectively. These assignments are extended below (part III) by analogy to sequential assignments previously obtained under acidic conditions (Kline & Justice, 1990; Boelens et al., 1990; Hua & Weiss, 1990, 1991) and by analysis of spatial relationships observed in crystal structures (Figure 1B; Blundell et al., 1971; Dodson et al., 1979; Baker et al., 1988).

(i) ^{13}C Labeling of GlyB23. In crystal structures residues B20–B23 form a (1 → 4) β-turn; the B-chain continues in an extended conformation. The B23 (ϕ, ψ) dihedral angles can only be accommodated by glycine (or D-amino acids), and glycine is conserved at this position. In the 2-Zn crystal a significant interaction is observed between GlyB23 and the side chain of Asn21 (Blundell et al., 1971; Peking Insulin Structure Group, 1971; Baker et al., 1988).

The two H_α resonances of GlyB23 are assigned by specific $^{13}C_\alpha$ labeling. The ^{1}H and ^{13}C NMR assignments of GlyB23-C_α are obtained by heteronuclear correlation (panel A of Figure 6; Table III). Only a pair of sharp doublets is

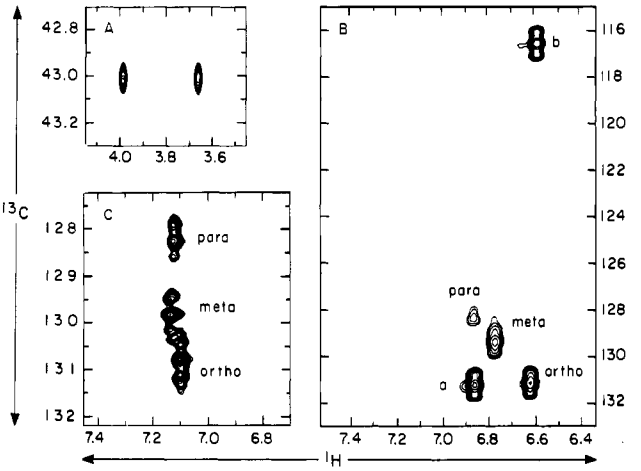

FIGURE 6: HMQC heteronuclear correlation spectra of ^{13}C-labeled DKP-insulins: (A) [$^{13}C_\alpha$]GlyB23 labeled DKP-insulin; (B) [*ring*-$^{13}C_5$]PheB25 labeled DKP-insulin; (C) [*ring*-$^{13}C_5$]PheB24 and [*ring*-$^{13}C_4$]TyrB26 labeled DKP-insulin. In panel C the B26 ortho cross-peak is labeled a and the meta cross-peak is labeled b, and the three B24 cross-peaks are labeled ortho, meta, and para. Each ring is observed to be in fast change on the ^{1}H and ^{13}C NMR time scales with respect to ring rotation. ^{13}C chemical shifts are measured in reference to dioxane (assumed to be at 67.8 ppm; Table III). Fine structure in the ^{13}C dimension is due to direct ^{13}C ^2J homonuclear coupling. In each spectrum a shifted Gaussian window function was applied in ω_2 and a cosine function was applied in ω_1.

observed in the edited 1D spectrum (Figure S2); their $^2J_{HH}$ connectivity is verified in the DQF-COSY spectrum (arrow in panel B of Figure 4). The narrow line widths of the GlyB23-C_α and -H_α resonances (relative to those of internal residues; see below) suggest significant segmental mobility. Such mobility is also evident in the absence of efficient cross-relaxation pathways; in the NOESY spectrum of DKP-insulin GlyB23 exhibits only a single, weak interresidue cross-peak (to neighboring PheB24; part III). A predicted tertiary interaction with AsnA21 is conspicuously absent.

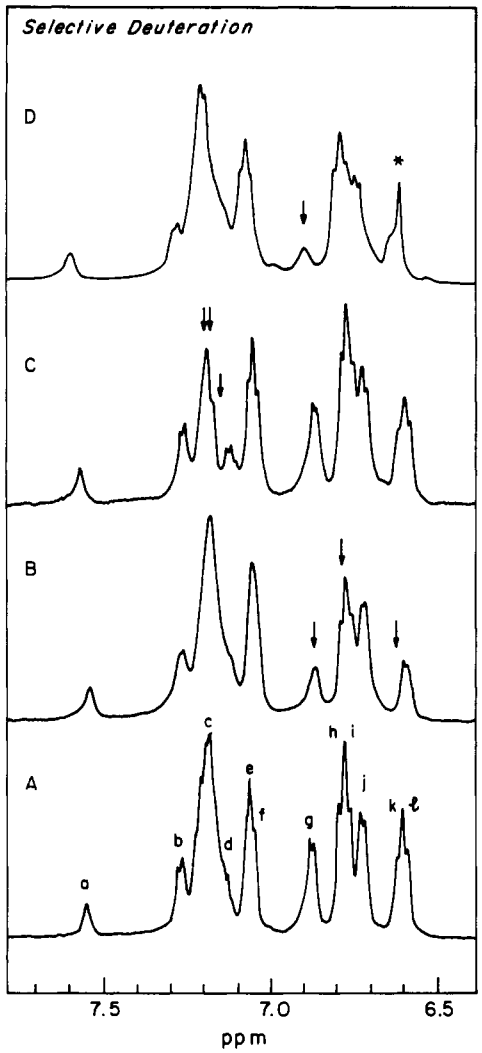

FIGURE 7: Aromatic region of 500 MHz ^{1}H NMR spectra of ^{2}H-labeled insulin analogue at pD 8.0 and 37 °C at 1.5 mM protein concentration: (A) unlabeled, (B) [*ring*-$^2H_5$]PheB24 insulin, (C) [*ring*-$^2H_5$]PheB25 insulin, and (D) [*ring*-$^2H_4$]TyrB26 insulin. Arrows indicate attenuation of proton resonances due to deuteration. The meta (ϵ) deuterons of TyrB26 were partially back-exchanged during HF cleavage of the labeled octapeptide (see Materials and Methods); the corresponding singlet resonance is indicated by an asterisk in panel D. The spectra were the sum of 128 scans. An exponential multiplication of 3 Hz was applied before Fourier transformation. Resonances a–l in panel A are labeled as described in the caption to Figure 3.

(ii) ^{2}H Labeling of Aromatic Residues B24, B25, and B26. Residues PheB24-PheB25-TyrB26 are generally conserved among vertebrate insulins. Mutations at positions B24 and B25 are associated with diabetes in man (Tager et al., 1979; Shoelson et al., 1983a,b; Haneda et al., 1984), and these residues may interact directly with the receptor (Pullen et al., 1976; Baker et al., 1988). The role of TyrB26 in receptor recognition is not clear; in its absence des-pentapeptide(B26–B30) insulin amide exhibits native bioactivity (Fisher et al., 1985, 1986; Nakagawa & Tager, 1986).

The aromatic resonances of B24, B25, and B26 are assigned by specific deuteration. The unlabeled aromatic ^{1}H NMR spectrum of DKP-insulin is shown in panel A of Figure 7. The spectrum of an analogue containing [*ring*-$^2H_5$]PheB24 insulin is shown in panel B; the spectrum of an analogue containing [*ring*-$^2H_5$]PheB25 is shown in panel C; the spectrum of an analogue containing [*ring*-$^2H_4$]TyrB26 is shown in panel D. In each case, resonance amplitude is selectively attenuated, as indicated by arrows in panels B–D. The (3′,5′) deuterons

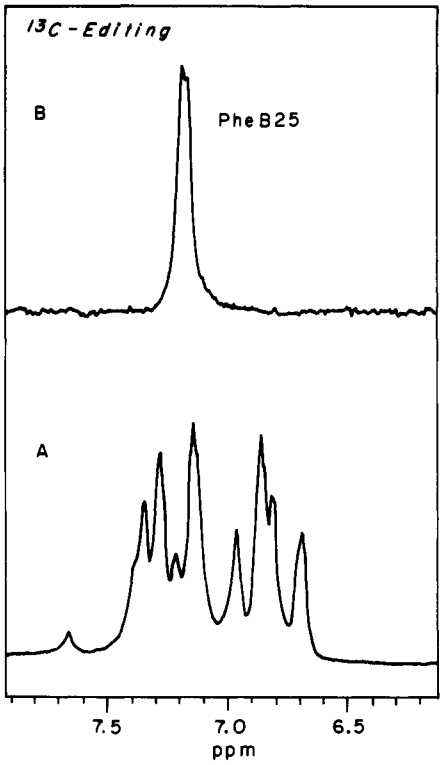

FIGURE 8: (A) Unedited aromatic ^{1}H NMR spectrum (decoupled) of DKP-insulin containing [*ring*-$^{13}C_5$]PheB25 at 25 °C and pD 8. (B) ^{13}C-Edited aromatic spectrum showing unresolved ring resonances at 7.11–7.18 ppm. The protein concentration was 1 mM; 128 scans were observed at 25 °C (small differences are observed relative to spectrum at 37 °C; Figure 3).

of [*ring*-$^2H_4$]TyrB26-labeled DKP-insulin were partially back-exchanged during HF cleavage of the labeled octapeptide (see Materials and Methods); the corresponding meta ($^1H_{(3-5)}$) singlet resonance is indicated by an asterisk in panel D. The aromatic spin systems are outlined in two dimensions in the TOCSY spectra (Figure S3). Deuteration of PheB25 leads to loss of unresolved intensity near the diagonal at 7.1–7.2 ppm.

(iii) ^{13}C-Labeling of Aromatic Rings. The absence of a clear B25 aromatic spin system may be due to degeneracy of the ortho, meta, and para chemical shifts. Alternatively, the B25 resonances may be broadened by intermediate exchange between two or more stable local environments. The latter mechanism is suggested by the observation of two distinct side-chain configurations in the crystallographic dimer (molecules 1 and 2; Peking Insulin Structure Group, 1971; Blundell et al., 1971; Baker et al., 1988). To distinguish between these possibilities, we have synthesized DKP-insulin containing [*ring*-$^{13}C_5$]PheB25. The ^{13}C-edited spectrum, shown in Figure 8, clearly indicates that the resonances of PheB25 are sharp but unresolved. Like GlyB23, few interresidue NOEs are observed involving PheB25 (part III). These findings strongly suggest that PheB25 is flexible in solution. There is no evidence for significantly populated alternative configurations in the solution monomer of DKP-insulin, as observed in crystallographic dimers. Flexibility of B25 as a surface residue has previously been demonstrated in the crystal structure of des-pentapeptide insulin (DPI) (Bi et al., 1984) and in 20% acetic acid solution (Weiss et al., 1989; Hua & Weiss, 1990, 1991). In Figure 6 are shown two-dimensional ^{1}H–^{13}C HMQC spectra of PheB25 (panel B) and PheB24 and PheB26 (panel C). In each case the respective ortho and meta ^{1}H and ^{13}C ring resonances are observed to be equivalent on the ^{1}H and ^{13}C NMR time scales; these results demonstrate the absence of significant barriers to (C_β–C_γ) ring rotation

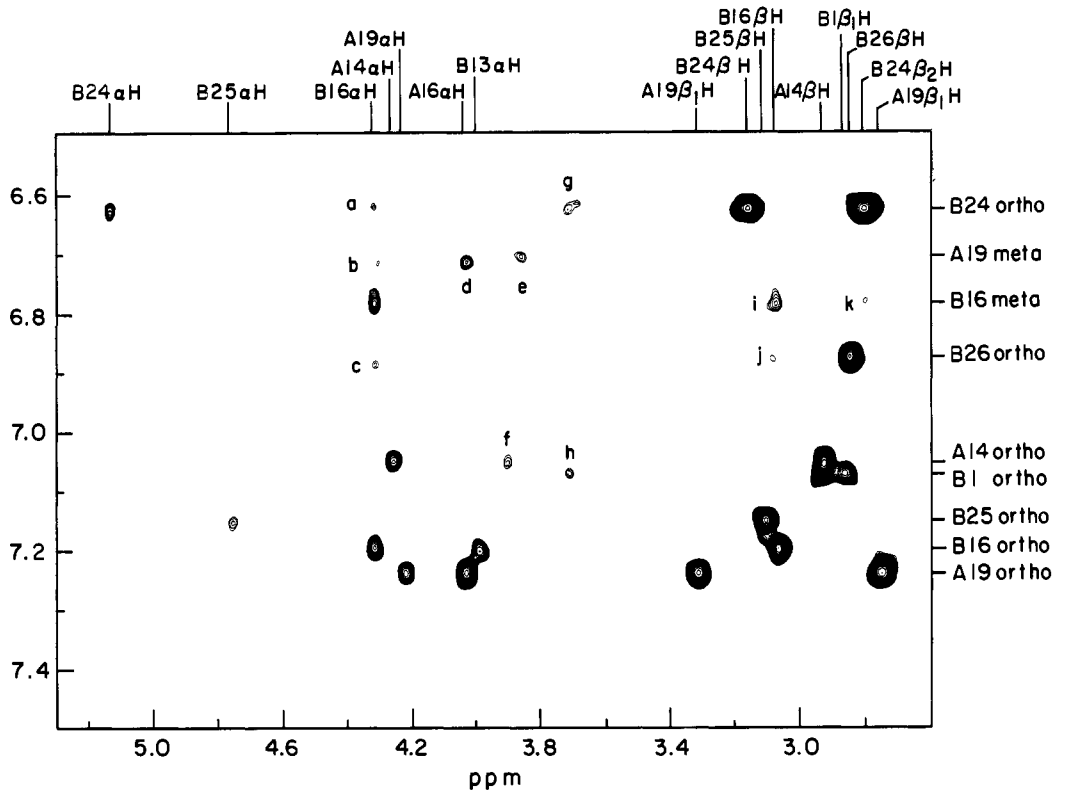

FIGURE 9: Assignment of H_α and H_β protons for aromatic residues based on intraresidue NOEs involving AMX spin systems. Interresidue cross-peaks a–k are discussed in the text. The data was recorded at 37 °C with a mixing time of 200 ms. The protein concentration was 0.75 mM. A total of 128 scans were observed per t_1 value. Exponential and shifted sine-bell window functions were applied in both dimensions; conditions were as described in the caption to Figure 4. The following cross-peaks are labeled: (a) B24-ortho/B16-H_α, (b) unassigned, (c) B26-ortho/B16-H_α (d) A19-meta/A16-H_α, (e) A19-meta/A2-H_α, (f) A14-ortho and unresolved H_α, (g) B24-ortho/B23-H_α2, (h) B1-ortho/unassigned, (i) B16-meta/B16-H_β and unresolved upper shoulder from A14-meta (unassigned), (j) B26-ortho/B16-H_β, and (k) B16-meta/B24-H_β.

in the solution structure. The resonances of PheB24 are broader than those of B25 and B26; more rapid T_2 relaxation also leads to relative attenuation of its three aromatic ^1H–^{13}C HMQC cross-peaks (Figure 6). The NOESY spectrum of DKP-insulin demonstrates that the B24 ring participates in multiple cross-relaxation pathways. These interactions provide probes for the structure of the hydrophobic core, as analyzed in detail below (part III).

(iv) Assignment of Remaining Aromatic Spin Systems. The spin system of PheB1 is assigned by elimination (resonances c, d, and e in Figure 3D). There is only one histidine (B5); its C_2H resonance at 7.6 ppm (pD 8.0) is labeled in Figure 3D. The C_4H resonance is identified in the TOCSY spectrum (data not shown). The remaining three aromatic spin systems (TyrA14, TyrA19, and TyrB16) are assigned below (part III) on the basis of nonlocal NOE patterns.

(III) Interresidue NOEs and Structural Implications

(i) Aromatic Spin Systems and Presumptive Tyrosine Assignments. Presumptive assignments of the three remaining unassigned tyrosine spin systems (A14, A19, and B16) are presented in turn. These assignments are based on NOE patterns to aliphatic protons (regions a and b in Figure 4D); these regions are shown in expanded form in Figures 9 and 10, respectively. Classification of methyl-containing spin systems is based on an analysis of the DQF-COSY and TOCSY data (panels B and C of Figure 4, respectively), and this classification is given in Table IV. Presumptive assignments of the aromatic residues are summarized in Table II.

The three remaining tyrosine spin systems exhibit distinctive NOESY interactions. (A) Of the unassigned tyrosine spin systems, one (ortho 7.04 ppm, meta 6.78 ppm; Table II) is distinguished by the absence of interresidue NOEs involving methyl resonances. This is assigned to TyrA14, which in crystal structures of insulin projects from the surface of the A-chain. A similar tyrosine spin system is observed in the spectrum of native insulin and DPI-insulin in acid/organic

Table IV: Classification of Methyl-Containing Spin Systems and Presumptive Assignment[a] at pH 8.0 and 37 °C

	residue	chemical shifts		
		$C^\alpha H$	$C^\beta H$	others
Leu	A (unassigned)	3.80	1.41, 1.47	$C^\gamma H$ 1.47
				$C^\delta H_3$ 0.78, 0.71
	B (A16)	4.01	1.85, 1.65	$C^\gamma H$ 1.68
				$C^\delta H_3$ 0.86, 0.83
	C (unassigned)	4.48	1.63, 0.69	$C^\gamma H$ 1.56
				$C^\delta H_3$ 0.74, 0.65
	D (B11)	3.81	1.69, 1.13	$C^\gamma H$ 1.15
				$C^\delta H_3$ 0.58, 0.56
	E (B15)	3.61	0.86, 0.11	$C^\gamma H$ 1.19
				$C^\delta H_3$ 0.45, 0.08
	F (B17)	4.00	1.87, 1.28	$C^\gamma H$ 1.65
				$C^\delta H_3$ 0.64, 0.64
Val	A (unassigned)	3.56	1.84	$C^\gamma H_3$ 0.81, 0.76
	B (B2)	3.89	1.84	$C^\gamma H_3$ 0.72, 0.67
	C (B12)	3.07	2.03	$C^\gamma H_3$ 0.91, 0.86
	D (unassigned)	3.65	1.87	$C^\gamma H_3$ 0.89, 0.75
Ile	A (A2)	3.86	1.19	$C^\gamma H_2$ 1.09. 0.82
				$C^{\gamma'} H_3$ 0.61, $C^\delta H_3$ 0.49
	B (A10)	4.09	1.49	$C^\gamma H_2$ 1.02, 0.36
				$C^{\gamma'} H_3$ 0.56, $C^\delta H_3$
Thr	A (unassigned)	4.04	4.30	$C^\gamma H_3$ 1.13
	B (unassigned)	4.29	3.98	1.05
	C (unassigned)	4.12	4.12	1.08

[a] Presumptive NOE-based assignments of aliphatic spin systems are indicated in parentheses and are not stereospecific.

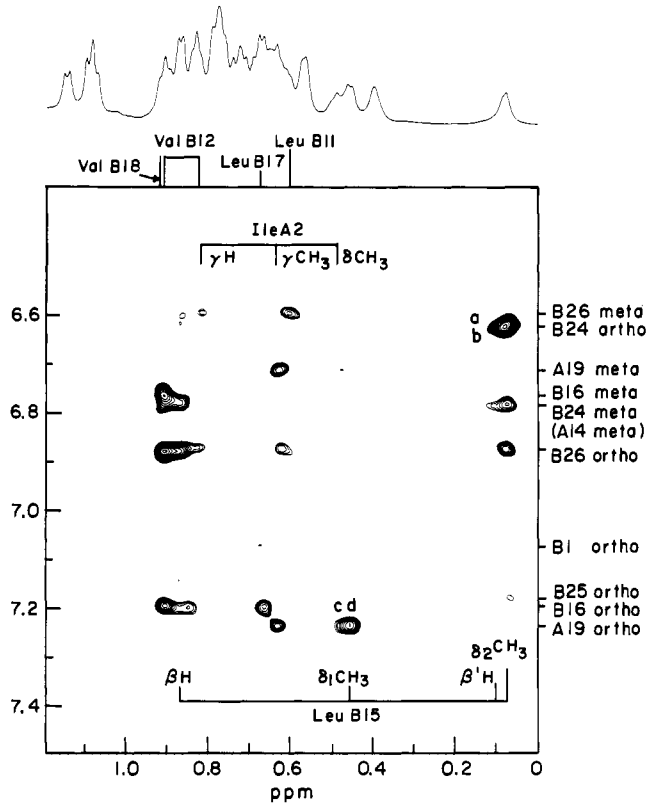

FIGURE 10: Aromatic–aliphatic NOEs in the NOESY spectrum at 37 °C. Presumptive methyl assignments are indicated on the basis of crystal structures and sequential ^{1}H NMR assignment under acidic conditions (Kline & Justice, 1990; Hua & Weiss, 1990). Overlapping cross-peaks between LeuB15 (horizontal axis) and B26-meta and B24-ortho are labeled a and b, respectively; overlapping cross-peaks between A19-ortho (vertical axis) and IleA2-δCH_3 and LeuB15-$\delta_1 CH_3$ are labeled c and d, respectively. The mixing time was 200 ms; conditions were as described in the caption to Figure 4.

cosolvents and assigned to A14 by chemical modification (Weiss et al., 1989) and by sequential methods (Kline & Justice, 1990; Boelens et al., 1990; Hua & Weiss, 1990, 1991). (B) Of the remaining two tyrosines, one (ortho 7.23 ppm, meta 6.70 ppm; Table II) is distinguished by NOEs involving an isoleucine spin system. This is assigned to TyrA19, which in crystal structures is near IleA2 (Baker et al., 1988). This presumptive assignment and long-range NOE is also in accord with previous 2D NMR studies of insulin and DPI-insulin conducted under acidic/mixed-organic conditions. (C) The remaining spin system (ortho 7.18, meta 6.74) is assigned to TyrB16 by elimination. Additional interresidue NOE patterns consistent with these assignments are discussed below (section iii). No NOEs are observed between aromatic rings (Figure 4D). The absence of NOEs between TyrA19 and PheB25 suggests that the latter side chain adopts an outward orientation (molecule 2; Peking Insulin Structure Group, 1971).

(*ii*) *Aromatic AMX Spin Systems.* The assignment of aromatic ring resonances may be extended to corresponding H_α, $H_{\beta 1}$, and $H_{\beta 2}$ resonances by NOESY cross-peaks involving AMX spin systems (as identified in DQF-COSY and TOCSY spectra; Figure 4). Region a of the NOESY spectrum is shown in Figure 9, and aromatic AMX assignments are indicated. In cases of similar chemical shifts, the aromatic resonance involved (vertical axis) is verified by corresponding NOESY spectra of the selectively deuterated analogues (part II). We note in passing that the absence of intraresidue cross-peaks between aromatic meta and H_β protons for internal rings A19 and B24 (see below) suggests that spin diffusion is negligible under conditions of study (100–200-ms mixing time and 37 °C). Additional NOESY cross-peaks in region a (labeled a–h in Figure 9) represent interresidue effects and are considered below.

(*iii*) *Local Environments of Aromatic Residues.* Interresidue NOEs may be used to map the local environments of the aromatic rings. Presumptive assignments of several aliphatic spin systems are obtained from this analysis as summarized in Table IV. The local environments of aromatic residues have previously been analyzed in crystal models by molecular mechanics calculations (Weiss et al., 1989).

HisB5. In crystal structures HisB5 packs near IleA10 within a solvent-exposed pocket between the A- and B-chains. The C_2H and C_4H protons of HisB5 indeed exhibit NOEs to an isoleucine spin system (δCH_3 0.39 ppm and γ' CH_3 0.56 ppm). The latter is distinct from that assigned above to IleA2 (on the basis of an NOE to TyrA19; section i). Since DKP-insulin contains only two isoleucines (Figure 2), the TyrA19 and HisB5 NOEs provide consistent assignments of IleA2 and IleA10, respectively. In further accord with crystal structures, IleA10 exhibits no NOEs with any tyrosine or phenylalanine spin systems (below).

PheB1. The configuration of the N-terminal residues of the B-chain varies widely among crystal structures, and flexibility in this region is suggested by molecular dynamics calculations (Kruger et al., 1987). There are no prominent NOEs between PheB1 and aliphatic spin systems; however, weak NOEs are observed between PheB1 and a valine spin system (Figure 9). The latter in turn exhibits weak interresidue NOEs involving an AMX spin system. It is possible (although not established) that this string of weak spatial relationships represents PheB1-ValB2-AsnA3. These residues are highly variable among known insulin sequences and not thought to be involved in receptor recognition. PheB1 has previously been inferred to be flexible in solution from circular dichroic (CD) studies of a des-PheB1 analogue (Wollmer et al., 1979) and from NMR relaxation studies in 20% acetic acid (Weiss et al., 1989; Hua & Weiss, 1990). An additional NOE involving the ortho resonance of PheB1 is observed (cross-peak h in Figure 9); it is not classified at this time due to resonance overlap. An analogous NOE is not observed in the spectra of human insulin (Kline & Justice, 1990; Hua & Weiss, 1991) or DPI (Hua & Weiss, 1990) in acid/organic cosolvents.

PheB24. The NOESY spectrum contains cross-peaks from PheB24 to four spin systems, belonging to (a) leucine, (b) valine, (c) tyrosine, and (d) glycine; these are discussed in turn.

(*a*) *B24-Leucine NOE.* An NOE is observed between an upfield-shifted leucine spin system (assigned presently to LeuB15) and both PheB24 and TyrB26 (Figure 10). The observed pattern of NOE intensities is in qualitative agreement with $\langle r^{-6} \rangle$-averaged interproton distances from B15 to neighboring aromatic rings in molecule 1 (Table V) and molecule 2 (Table VI and Figure 1B) of the 2-Zn crystal structure (Chinese nomenclature; Baker et al., 1988). A presumptive assignment of LeuB15 was obtained by analogy to the sequential assignment of insulin and des-pentapeptide insulin (DPI) in mixed acid/organic solvent systems (Kline & Justice, 1990; Hua & Weiss, 1990, 1991). In each spectrum a similar NOE is observed between an upfield-shifted leucine spin system and PheB24 (TyrB26 is absent in DPI, which lacks residues B26–B30). A similar assignment of an upfield-shifted methyl resonance has been proposed by Roy et al. (1990) in the spectrum of the AspB9-insulin analogue.

The spin system of LeuB15 is outlined in the enlarged TOCSY spectrum shown in Figure 11. Remarkably, a leucine β-proton is shifted to 0.11 ppm (dashed line), overlapping the

Table V: $\langle r^{-6} \rangle$-Averaged Interproton Distances[a] (<5 Å) between LeuB15 and IleA2 and Nearest Aromatic Rings in 2-Zn Structure (Molecule 1; Chinese Nomenclature)

	TyrA19		TyrB16		PheB24			PheB25			TyrB26	
proton	ortho	meta	ortho	meta	ortho	meta	para	ortho	meta	para	ortho	meta
IleA2												
H_α	5.5	**3.9**	>10	>10	>10	>10	>10	9.4	8.5	8.8	7.5	7.4
H_β	**4.1**	**3.5**	>10	>10	8.5	9.6	10.9	6.8	6.3	7.0	5.4	6.2
$H_{\gamma 1}$	**3.8**	**3.2**	>10	>10	>10	>10	>10	>10	>10	>10	6.1	6.7
$H_{\gamma 2}$	5.4	**4.9**	>10	>10	>10	>10	>10	>10	>10	>10	5.3	5.2
$H_\gamma CH_3$	5.8	5.6	>10	>10	>10	>10	>10	>10	>10	>10	**3.4**	**3.7**
$H_\delta CH_3$	**4.0**	**4.9**	>10	>10	6.6	7.3	8.5	>10	>10	>10	**3.3**	**4.5**
LeuB15												
H_α	6.8	8.9	7.4	9.6	5.6	6.2	6.4	>10	>10	>10	8.5	9.6
$H_{\beta 1}$	7.0	9.2	6.8	9.2	**3.7**	**4.1**	**4.4**	8.4	9.3	9.7	6.7	8.7
$H_{\beta 2}$	7.6	9.6	6.9	9.3	**4.7**	**4.3**	**4.1**	9.7	>10	>10	6.3	7.7
H_γ	5.7	7.4	9.0	>10	6.1	6.1	6.4	9.4	9.8	9.9	5.9	7.2
$H_{\delta 1}CH_3$	5.8	7.4	9.2	>10	**3.5**	**4.0**	**4.8**	7.5	8.5	8.8	**3.7**	5.6
$H_{\delta 2}CH_3$	**3.9**	5.7	9.3	>10	**4.7**	6.1	6.8	7.7	7.9	7.9	6.5	7.8

[a] Proton coordinates were extrapolated from the heavy atom coordinates (Blundell et al., 1971) with the use of the CHARRM program developed by Karplus and colleagues (Brooks et al., 1983). Distances corresponding to nonnegligible NOEs (<5 Å) are shown in boldface.

Table VI: $\langle r^{-6} \rangle$-Averaged Interproton Distances[a] (<5 Å) between LeuB15 ad IleA2 and Nearest Aromatic Rings in 2-Zn Structure (Molecule 2; Chinese Nomenclature)

	TyrA19		TyrB16		PheB24			PheB25			TyrB26	
proton	ortho	meta	ortho	meta	ortho	meta	para	ortho	meta	para	ortho	meta
IleA2												
H_α	6.9	5.4	>10	>10	>10	>10	>10	>10	>10	>10	9.4	9.3
H_β	**4.6**	**3.0**	>10	>10	8.5	9.6	10.9	>10	>10	>10	8.5	9.0
$H_{\gamma 1}$	5.6	5.1	>10	>10	>10	>10	>10	>10	>10	>10	7.7	7.7
$H_{\gamma 2}$	**3.7**	**3.4**	>10	>10	9.6	>10	>10	>10	>10	>10	8.0	8.6
$H_\gamma CH_3$	**4.3**	**4.0**	>10	>10	8.5	9.7	>10	>10	>10	>10	5.9	6.5
$H_\delta CH_3$	5.6	**3.9**	>10	>10	>10	>10	>10	>10	>10	>10	>10	>10
LeuB15												
H_α	7.5	9.7	7.4	9.6	5.6	6.0	6.2	>10	>10	>10	8.0	9.5
$H_{\beta 1}$	7.3	9.5	6.7	9.1	**3.6**	**3.9**	**4.0**	9.1	>10	>10	6.2	8.1
$H_{\beta 2}$	8.2	6.5	6.9	9.4	**4.7**	**4.1**	**3.9**	>10	>10	>10	5.6	7.0
H_γ	6.5	8.2	9.1	>10	5.8	5.9	6.2	>10	>10	>10	5.5	6.3
$H_{\delta 1}CH_3$	5.9	7.5	9.2	>10	**3.4**	**3.9**	5.1	8.7	>10	>10	**3.7**	5.1
$H_{\delta 2}CH_3$	**4.8**	6.9	9.2	>10	**4.8**	6.1	6.7	6.7	>10	>10	6.5	8.3

[a] Proton coordinates were extrapolated from the heavy atom coordinates (Blundell et al., 1971) with the use of the CHARRM program developed by Karplus and colleagues (Brooks et al., 1983). Distances corresponding to nonnegligible NOEs (<5 Å) are shown in boldface.

resonance of the related leucine δ_2CH_3 resonance at 0.08 ppm (solid line; assignment not stereospecific). This large secondary shift is presumably due to the ring currents of PheB24 and/or TyrB26 (Johnson & Bovey, 1958; Perkins & Dwek, 1980; Hoch et al., 1982). Although the B24-leucine and B26-leucine cross-peaks overlap, their relative contributions are resolved by selective deuteration (part III; data not shown). A composite cross-peak is observed between the Leu-δ_2CH_3 and -β resonance (horizontal axis in Figure 10) and the PheB24-ortho resonance (major cross-peak b) and the TyrB26-meta resonance (minor shoulder labeled a). These NOEs are stereospecific; i.e., no cross-peak is observed to the other Leu-δ_1CH_3 resonance at 0.45 ppm. The A19-ortho/Leu-δ_2CH_3 NOESY cross-peak is stronger than that involving the meta resonance, whereas the B26-ortho and -meta resonances exhibit B15 NOEs of similar strength. Similarly, an NOE is observed between the 0.45-ppm Leu-δ_1CH_3 resonance and the ortho (but not meta) proton and one (but not the other) β-proton of TyrA19. Such a precise pattern of stereospecific NOEs indicates that the hydrophobic core of DKP-insulin is well-ordered in this region.

We note in passing that the DPI data (Hua & Weiss, 1990) suggest that the major contribution to the upfield secondary shift of LeuB15 is due to PheB24 rather than TyrB26. Ring-current shift calculations, based on crystal models of native insulin, support this conclusion (Table VII; predicted

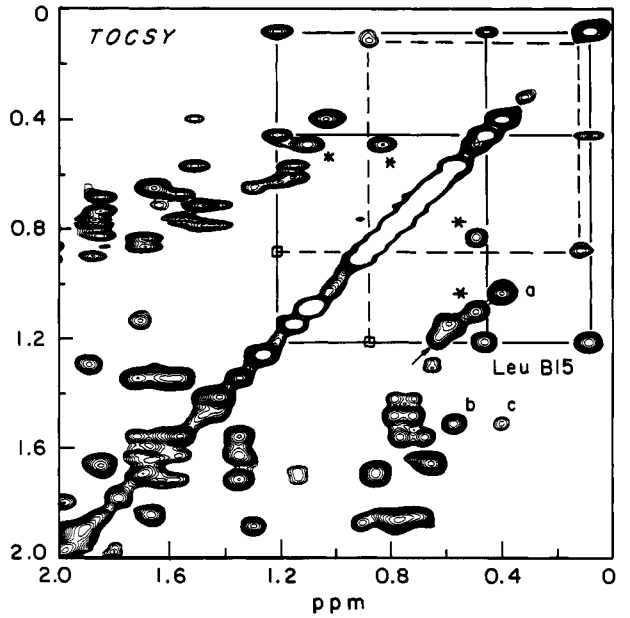

FIGURE 11: Upfield portion of the TOCSY spectrum (panel C of Figure 4). The LeuB15 spin system is outlined by solid (δ_2CH_3 at 0.08 ppm) and dashed (H_β at 0.11 ppm) lines. IleA2 cross-peaks [from δCH_3 (0.49 ppm) to the two H_γ resonances (at 1.09 and 0.82 ppm)] are indicated by asterisks. The mixing time was 55 ms at 37 °C; conditions were as described in the caption to Figure 4.

Table VII: Calculated Ring-Current Shifts for LeuB15[a]

residue	ring	A14	A19	B1	B5	B10	B16	B24	B25	B26	total
LeuB15	H_α	0.01	−0.03	0.03	0.00	−0.01	−0.02	**0.30**	0.05	0.00	0.33
	H_β	0.01	0.00	0.01	0.00	0.00	−0.05	**0.92**	0.05	0.03	0.97
	$H_{\beta'}$	0.01	−0.02	0.01	0.00	0.00	−0.04	**1.96**	0.07	0.00	1.99
	H_γ	0.01	0.01	0.01	0.00	−0.01	−0.02	**0.26**	0.06	−0.01	0.16
	$H_{\delta 1}CH_3$	0.00	0.06	0.01	0.00	0.00	−0.02	**0.18**	0.09	−0.07	0.25
	$H_{\delta 2}CH_3$	0.00	−0.09	0.02	0.00	0.00	−0.01	**0.18**	0.13	−0.03	0.20

[a] Ring-current calculations were performed as previously described (Hoch et al., 1982; Weiss & Hoch, 1987), assuming the 2-Zn crystal structure of porcine insulin; the two protomers (molecules 1 and 2) yielded essentially similar results.

ring-current effects of other methyl-containing spin systems are provided in Table S1). This conclusion is in accord with recent NMR studies of DKP-insulin analogues in which one ring or the other is absent, i.e., AspB10-DPI and [PheB24 → Gly]DKP-insulin (Q.X.H., S.E.S., and M.A.W., unpublished results).

(*b*) *B24-Valine NOE.* Of the four valine residues in DKP-insulin, one exhibits NOEs with PheB24, TyrB26, and TyrB16 (Figure 10). This involves the H_α (3.07 ppm) and γ_1CH_3 (0.91 ppm) and is assigned to ValB12 on the basis of the crystal structure (Figure 1B). In the spectrum of DPI in 20% acetic acid, an NOE is observed from ValB12 to PheB24 but not to TyrB16 (Hua & Weiss, 1990). Interestingly, an (i, i + 3) NOE is observed between ValB12-H_α and LeuB15-δ_2CH_3 (0.08 ppm; see above). This NOE provides a check on the consistency of the two presumptive assignments and also suggests that an α-helical configuration is retained in this region. The ValB12-H_α resonance (but not the methyl resonances) exhibits a significant upfield secondary shift. Comparative studies of insulin analogues suggest that this shift, like that of B15, is due to the ring current of PheB24 (Boelens et al., 1990; Hua & Weiss, 1990; unpublished results) in accord with ring-current shift calculations (supplementary material).

(*c*) *B24-Tyrosine NOE.* Additional interresidue NOEs are observed between the ring protons of PheB24 and the H_α proton of TyrB16 (Figure 9). Their proximity presumably reflects the $\beta(1 \rightarrow 4)$ turn between residues B20 and B23, an invariant feature of insulin in otherwise different crystal forms (Blundell et al., 1971; Bentley et al., 1976; Bi et al., 1984; Baker et al., 1988). The TyrB16-H_α cross-peak involving the B24-ortho protons is labeled a in Figure 9, and the cross-peak involving the B24-para proton is labeled c. The relationship between the B24 and B16 residues is further defined by an NOE between a B24 β-proton and the TyrB16-meta resonance (cross-peak k in Figure 9). (We note in passing that since the B24-para and B26-ortho resonances are not resolved (Figure 7), the potential ambiguity in the assignment of cross-peak c in Figure 9 must be resolved by selective deuteration as described in part II. Similarly, the cross-peak involving the B24-meta resonance partially overlaps the intraresidue NOE between B16-H_α and its meta protons. Resolving such cross-peak overlaps illustrates the utility of selective isotopic labeling.)

(*d*) *B24-Glycine NOE.* A weak NOE is observed between the B24-meta resonance and an H_α of GlyB23 (cross-peak g; assigned by ^{13}C labeling in part II).

PheB25. No prominent interresidue NOEs are observed involving the unresolved B25 ring protons at 7.11–7.18 ppm. This is an important negative result. As discussed above (part II(iv)), in the crystallophic dimer PheB25 assumes two asymmetric configurations, inward [packing against TyrA19; molecule 1 of the 2-Zn structure (Chinese nomenclature)] and outward (molecule 2; residue d in Figure 1A). In DKP-insulin no NOE is observed between the ring of PheB25 and the H_α or H_β protons of TyrA19, as would be expected in molecule 1 (Blundell et al., 1971; Peking Insulin Structure Group, 1971). An outward configuration for PheB25 has previously been shown for insulin and DPI in 20% acetic acid (Weiss et al., 1989; Hua & Weiss, 1990, 1991), although a weak B25–A19 NOE has recently been described in DPI at pH 1.8 (Boelens et al., 1990). An outward configuration would enable PheB25 to interact directly with the insulin receptor, as suggested by comparative studies of insulin analogues (Nakagawa & Tager, 1986; Mirmira & Tager, 1989) and direct photo-cross-linking of insulin and the insulin receptor (S.E.S., unpublished results). A weak NOE is observed between the ring resonances of PheB25 and LeuB15-δ_2CH_3; a similar NOE has been observed in DPI in 20% acetic acid (Hua & Weiss, 1990, 1991) and ascribed to the transient excursion of a flexible side chain (B25) near a stable side chain (B15).

TyrA14. Although there are no major cross-peaks involving the A14 ring, a weak NOE (cross-peak f in Figure 9) is observed between the ortho resonance of TyrA14 (7.04 ppm). The target spin system cannot be unambiguously classified, as overlap occurs at this position between a long-chain spin system (H_α), a valine spin system (H_α), and an AMX spin system (H_β). The absence of NOEs involving methyl resonances is consistent with the surface location of this residue (i.e., TyrA14 is not part of the hydrophobic core). Exposure of the TyrA14 ring to solvent has previously been demonstrated under a variety of conditions by photochemically induced dynamic nuclear polarization (photo-CIDNP; Kaptein, 1980; Muszkat et al., 1984; Weiss et al., 1989).

TyrA19. Significant NOEs are observed between the A19 ring protons and two sets of aliphatic protons; these belong to (a) isoleucine and (b) leucine spin systems.

(*a*) *A19-Isoleucine NOE.* As discussed above, NOEs are observed between the $\gamma'CH_3$ group of an isoleucine (0.61 ppm) and both ring protons of TyrA19 (Figure 10); weaker NOEs are observed involving the δCH_3 group (0.49 ppm). An NOE is also observed between an H_γ (0.82 ppm) and $\gamma'CH_3$ of Ile2 and the ortho resonance of TyrB26. The isoleucine involved may be consistently assigned to IleA2 (part IV(i)). A similar set of NOEs is observed in the NOESY spectrum of DPI (exclusive of B26) and assigned by sequential methods to IleA2 (Hua & Weiss, 1990). IleA2 and TyrA19 are strictly conserved among known insulins and insulin-related sequences, and their interaction (shown in Figure 1B) appears to be a defining feature of the insulin fold (Baker et al., 1988).

(*b*) *A19-Leucine NOE.* An NOE is also observed between the ring resonances of TyrA19 and the H_α of a leucine spin system (Figure 9); the NOE involving the ortho protons is approximately 15 times larger than that involving the meta protons. A similar set of cross-peaks is observed in the NOESY spectrum of DPI and assigned by sequential methods to LeuA16 (Hua & Weiss, 1990). In crystal structures these protons, located in the C-terminal α-helix of the A-chain, are 2–4 Å apart (Figure 1B); consistent with relative NOE intensities, an A19-ortho proton is predicted by crystal structures

to be 1–2 Å closer to LeuA16-H_α than the nearest meta proton. However, an (i, i + 3) helix-related NOE predicted to occur between LeuA16-H_α and a β-proton of Tyr19 is not observed; the significance of its absence is not clear.

TyrB16. An NOE between the B16 meta resonance and a B24 β-proton is described above (cross-peak k in Figure 9). An additional interresidue NOE is also observed between the ortho resonance of TyrB16 and (a) the H_α of an unassigned leucine and (b) the H_α of a long-chain spin system. The former may be assigned to LeuB17 (the succeeding residue on the surface of the putative B-chain α-helix) and the latter to GluB13-H_α [a (1, 1 + 3) helix-related residue]. Analogous cross-peaks are observed in the NOESY spectrum of DPI and insulin in 20% acetic acid (Hua & Weiss, 1990, 1991). Interestingly, TyrB16 (unlike internal rings A19 and B24) exhibits intraresidue NOEs to H_α and H_β protons from its meta as well as ortho ring resonances. This is likely to reflect local mobility of the side chain in accord with the high crystallographic B-factors observed for this residue (Baker et al., 1988).

TyrB26. NOEs between B26 and IleA2, LeuB15, and ValB12 are described above. These NOEs demonstrate that the B26 ring is packed against the hydrophobic core as observed in crystal structures; i.e., the C-terminal region of the B-chain is tethered to the protein at least at this point. Such tethering has been the subject of considerable speculation (Dodson et al., 1983; Mirmira & Tager, 1989) and has implications for models of insulin action (Baker et al., 1988).

An additional NOE is observed between the meta resonance of TyrB26 and a previously unassigned leucine (δCH_3 0.56/0.58 ppm). As was described for the B26 and B24 interactions with B15 and B12 (see above), this NOE is stereospecific; i.e., only one of the methyl resonances exhibits a nonnegligible NOE, and only to the B26-meta (not ortho) resonance (Figure 10). This leucine is assigned on the basis of crystal structures to LeuB11; the proximity of B26 and B11 reflects the $\beta(1 \rightarrow 4)$ turn in the B-chain between residues B20 and B23. An (i, i + 4) NOE is observed between LeuB15-δ_2CH_3 and the H_γ and both methyl resonances of LeuB11 (data not shown). This NOE, also predicted by crystal structures (Figure 1B), provides a consistency check on the two leucine assignments. Interestingly, no NOE is observed between B26 and an additional valine spin system; such an NOE might be expected involving ValA3, but this interchain interaction is not a consistent feature in different crystal forms.

Discussion

The physiologically active form of insulin is the monomer, and the self-association surfaces of insulin may be redesigned without loss of bioactivity (Brange et al., 1988, 1990). The primary objective of this paper is to demonstrate the feasibility of detailed 2D NMR studies of an engineered insulin monomer (DKP-insulin) in aqueous solution in the physiological pH range. Although such studies of native insulin are limited by aggregation, this limitation is circumvented through the use of specific amino acid substitutions on the surface of the protein (Figure 1A).

DKP-insulin contains three amino acid substitutions that alter the two principal surfaces of insulin involved in self-association: HisB10 → Asp, which destabilizes the hexamer interface, and [ProB28 → Lys; LysB29 → Pro], which destabilizes the dimer interface. Comparative studies of native human insulin and three essentially equipotent analogues—(i) the singly substituted analogue AspB10-insulin, (ii) the doubly substituted analogue KP-insulin, and (iii) DKP-insulin—demonstrate progressive reduction in concentration-dependent broadening of ^1H NMR resonances, as expected from the results of analytical ultracentrifugation (Table I). Rational design of insulin analogues with altered self-association properties was pioneered by Brange, Dodson, and colleagues and may have applications in medical therapeutics (Brange et al., 1990; Kang et al., 1990). The advantage of such analogues in ^1H NMR studies was first demonstrated by Dunn and co-workers in one-dimensional studies of AspB9-insulin at pH 8.0 (Roy et al., 1990). Sequential assignment of an AspB9 dimer at pH 1.8 has also been described (Kristensen et al., 1991).

(I) DKP-Insulin and IGF-1: Use of Homologous Sequences in Protein Design

DKP-insulin contains three substitutions [HisB10 → Asp; ProB28 → Lys; LysB29 → Pro], which introduce certain features of IGF-1. Although highly homologous to insulin, IGF-1 does not form insulin-like dimers or hexamers. Accordingly, it would be expected that chimeric analogues could be designed with selected properties of one or the other hormone. Although the crystal structure of IGF-1 has not been determined, its conformation is thought to resemble insulin, and a detailed model has been proposed (Blundell & Humbel, 1980). Insulin crystals exhibit an intricate set of protein–protein contacts, including discrete dimer- and hexamer-related surfaces. We discuss these surfaces in turn as a basis for protein design.

Dimer Contact. The insulin dimer contact is composed (in part) of an antiparallel β-sheet between residues B24 and B26 and is remarkable for an extensive set of van der Waals interactions between adjoining hydrophobic surfaces. IGF-1 does not form this dimer, and its sequence in this region differs from that of insulin in two sites whose structural consequences have been investigated by mutagenesis. First, contiguous aromatic residues PheB24-PheB25-TyrB26 in insulin are Phe23-Tyr24-Phe25 in IGF-1, and this difference is conserved among the vertebrate species. The corresponding PheB24-TyrB25-PheB26 insulin analogue has been constructed; its receptor-binding and dimerization properties are similar to those of native insulin (unpublished results). Second, the residues ProB28-LysB29 in human insulin are Lys27-Pro28 in IGF-1. Although insulin residues ProB28-LysB29 are observed in many of known insulins, they are not strictly conserved (Steiner et al., 1989) and may be altered without affecting receptor-binding potency. As originally demonstrated by Lilly Research Laboratories, the IGF-1-derived "swap" of residues B28 and B29 (i.e., [ProB28 → Lys; LysB29 → Pro]) reduces specific dimerization by at least 10^3-fold. The structural basis for this effect is presently not understood.

Hexamer Contact. The imidazole ring of HisB10 is responsible for zinc coordination in Zn^{2+} hexamers and also participates in the hexamer contact of non-zinc hexamers. The corresponding IGF-1 residue is Glu; hagfish insulin, which also does not form hexamers, contains Asp at this position. Studies of AspB10-insulin (human insulin) were originally motivated by the identification of Asp-B10-proinsulin in association with diabetes mellitus and hyperproinsulinemia in man (Grappuso et al., 1984; Chan et al., 1987). The mutation apparently impairs the regulated pathway of proinsulin processing, storage, and release (Carrol et al., 1988; Gross et al., 1989). The corresponding AspB10-insulin analogue was first synthesized by Katsoyannis and colleagues (Schwartz et al., 1987) and shown to exhibit enhanced bioactivity. Its effects on insulin binding and self-association, both alone and in combination with second-site mutations, were explored by Brange et al. (1988) and Schwartz et al. (1989). These studies suggest that modifications at positions B10 and B24–B30 may be

regarded as independent design features, a conclusion in accord with the present NMR studies.

(II) DKP-Insulin as 2D NMR Model System: Semisynthetic Labeling of the Receptor-Binding Surface

NMR Characterization of a Series of Analogues. DKP-insulin is monomeric and stably folded at the concentrations and conditions required for 2D NMR study in aqueous solution (pH 6–8). Accordingly, its ^{1}H NMR spectrum is well-resolved with the narrow line widths expected of a 6-kDa globular protein (such as bovine pancreatic trypsin inhibitor; Wagner & Wuthrich 1982); these features make possible the application of 2D pulse experiments (Wuthrich, 1986). A dramatic improvement is indeed observed in the quality of the 2D DQF-COSY and TOCSY spectra of DKP-insulin relative to native insulin. The requisite number of amino acid spin systems may be distinguished in these spectra, and nonlocal interresidue contacts may be resolved in the NOESY spectrum. Interestingly, the overall number of nonlocal NOESY cross-peaks is significantly less than that expected on the basis of static crystal models, suggesting quenching of some interresidue NOEs due to local dynamics. Since different crystallographic protomers predict distinguishable sets of interresidue NOEs—none of which are observed in toto—we speculate that the solution structure of DKP-insulin may differ from any one crystal form but span the range of different forms. Evidence for such global flexibility is considered below.

Amide Resonances and Conformational Flexibility. The amide ^{1}H NMR spectrum of DKP-insulin is remarkable for two features. (i) Base-catalyzed exchange of amide resonances occurs in much of the protein on a millisecond time scale, and no slowly exchanging amide resonances are observed in D_2O. On a technical level this time scale is too rapid to permit observation in H_2O of a complete set of H_N–H_α "fingerprint" cross-peaks, limiting complete assignment by conventional sequential methods (Wuthrich, 1986). More fundamentally, the rapid kinetics of amide proton exchange indicates global flexibility in the solution structure. Such flexibility has previously described on this basis in des-pentapeptide(B26–B30) insulin (DPI) at pH 1.8 (Boelens et al., 1990); the present results extend this observation to neutral pH. Complementary observations regarding rates of aromatic ring rotation are discussed below. (ii) Independent of solvent exchange, a large variation is observed in the line widths of amide resonances. Such variation has previously been described in the spectrum of native human insulin and DPI in mixed acid/organic solvents (Weiss et al., 1989; Kline & Justice, 1990; Hua & Weiss, 1990, 1991) and ascribed to intermediate exchange among conformational substates. Insulin and DPI retain native secondary structure under such conditions, and it is likely that such substates reflect millisecond displacements of elements of secondary structure, as inferred from an analysis of the structure of insulin in different crystal forms (Chothia et al., 1983). The present results at physiologic pH suggest that such motions are an intrinsic feature of the insulin fold (in the monomeric state) and are not dependent on the particular conditions of study. The question of an α-helical transition involving residues B1–B8 in an insulin monomer (corresponding to the T $\rightarrow$ R transition in insulin hexamers; Derewenda et al., 1989) is not addressed in the present study.

Isotope-Aided NMR Studies. As a first step to circumvent difficulties associated with conventional sequential assignment methods, assignment of key residues in the putative receptor-binding surface (Pullen et al., 1976; Baker et al., 1988) has been obtained by selective isotopic labeling. Modification and isotopic labeling of insulin at positions B23–B30 is readily accomplished by semisynthesis (Inouye et al., 1979, 1981a,b, 1983; Nakagawa & Tager, 1986). We have examined ^{2}H- and ^{13}C-labeled insulins at residues B23–B26 in DKP-insulin. These labels provide a rigorous assignment method and permit a focused analysis of NOESY interactions at the labeled sites. Implications concerning the solution structure and dynamics of (i) the hydrophobic core and (ii) the receptor-binding surface are discussed in turn.

(*i*) *Hydrophobic Core.* Interresidue NOESY cross-peaks indicate the spatial proximity between the B24 and B26 aromatic rings and other residues in the folded state of the protein. These patterns enable isotope-based assignment of residues B23–B26 to be extended to unlabeled sites by analogy with previously obtained sequential assignments under acidic conditions (Boelens et al., 1990) or in mixed acid/organic solvent systems (Kline & Justice, 1990; Hua & Weiss, 1990); corresponding spatial relationships are analyzed in reference to crystal models (Figure 1B). Although de novo structure determination by NMR requires an analysis of amide protons, the observed interresidue NOEs in D_2O reflect the maintenance of four conserved features of the insulin fold—the β(1 $\rightarrow$ 4) turn and central α-helix of the B-chain, the proximity of the N- and C-terminal regions of the A-chain, and the C-terminal α-helix of the A-chain.

(*ii*) *Receptor-Binding Surface.* The putative receptor-binding surface of insulin has been defined by comparative studies of analogues and species variants (Pullen et al., 1976). As projected onto crystallographic protomers, these residues span a contiguous surface of the protein, which contains a hydrophobic face and functional groups capable of specific hydrogen bonding (Baker et al., 1988). Aspects of this surface, such as that contributed by the central B-chain α-helix, are apparently recognized as a rigid unit by the receptor. Other elements may be flexible, however, and conformational flexibility may be required for high-affinity receptor binding (Nakagawa & Tager, 1986, 1987; Baker et al., 1988).

The C-terminal region of the B-chain has attracted particular attention due to observations of anomalous receptor-binding properties in a series of insulin and DPI analogues at positions B24 and B25 (Nakagawa & Tager, 1986, 1987; Mirmira & Tager, 1989). As noted above, residues B24–B26 form an antiparallel β-sheet in crystallographic dimers (Blundell et al., 1971; Peking Insulin Structure Group, 1971; Baker et al., 1988); the structure of this region in the monomer has not been determined. It is proposed that a conformational hinge may operate in this region, leading to a conformational change in receptor binding (Dodson et al., 1979, 1983; Mirmira & Tager, 1989).

The present NMR studies of DKP-insulin clearly demonstrate that the C-terminal region of the B-chain (residues B23–B30) remains tethered to the remainder of the protein in an engineered monomer. NOESY interactions indicate that PheB24 and TyrB26 each pack against the hydrophobic core, as observed in crystal structures (Blundell et al., 1971; Peking Insulin Structure Group, 1971; Baker et al., 1988). The absence of appreciable cis–trans isomerization in ProB29 also suggests a stable local structure. Since B28 and B29 are sites of mutation (Figure 2), no direct crystallographic information is available concerning their interactions.

The NMR data also indicate a degree of flexibility in the B23–B30 region. The side-chain resonances of PheB25 exhibit narrow ^{1}H and ^{13}C line widths (relative to PheB24 and TyrB26), suggesting that it is disordered. No significant interresidue NOEs are observed; in particular, the B25–A19 NOEs predicted by molecular 1 of the 2-Zn crystal structure

(Chinese nomenclature; Peking Insulin Structure Group, 1971) are absent. An outward orientation for PheB25 (molecule 2 of the 2-Zn structure) is suggested by the present results and would enable this side chain to interact directly with the insulin receptor. A very weak NOE observed with LeuB15 is likely to represent a transient excursion of the side chain (i.e., in a subset of the ensemble of solution structures; Torda et al., 1990) rather than a stable but distant interaction; such effects may in the future be modeled by molecular dynamics simulations (Kruger et al., 1987). The GlyB23-H_α resonances also exhibit very narrow line widths and an absence of significant interresidue NOEs; these features suggest segmental mobility in the β-turn. Interestingly, no NOE is observed to an AMX spin system, in particular to that of AsnA21. The absence of this interaction further suggests that the proximity of these two conserved residues—as observed in crystal structures—is not stably maintained in solution. Fluctuations in the B23–A21 distance have been modeled by molecular dynamics simulations (Kruger et al., 1987; D. Nguyen, M.A.W., and M. Karplus, unpublished results) and reflect both local motions of the A21 side chain and the global changes in the orientation of the C-terminal helix of the A-chain relative to the B-chain. Such global fluctuations may underlie the rapid kinetics of solvent exchange observed in DKP-insulin and anomalous broadening of amide resonances described in this and previous studies (Weiss et al., 1989, 1990; Kline & Justice, 1990).

How do the present results bear on the notion of a structural switch in the B24–B30 region? Although it is remarkable that this region remains tethered to the hydrophobic core in the absence of the dimer-related β-sheet, the presence or absence of these interactions does not directly demonstrate their relevance to receptor recognition. Although stably maintained in the monomer, for example, the B24 and B26 interactions with the hydrophobic core may be broken in the hormone–receptor complex (Dodson et al., 1983; Baker et al., 1988), as suggested by the anomalous receptor-binding properties of certain B24 and B25 mutations (Nakagawa & Tager, 1986, 1987) and the retention of bioactivity of des-pentapeptide-(B26–B30) insulin amide (Fisher et al., 1985; Nakagawa & Tager, 1986). Indeed, the substitutions PheB24 → D-Ala or D-Phe, which might be expected to destabilize the hydrophobic core, paradoxically enhance affinity for the insulin receptor (Kobayashi et al., 1982a,b; Mirmira & Tager, 1989). Comparative 2D NMR studies of monomeric analogues containing these and related substitutions will be required in the future to evaluate the relative importance of flexible and rigid elements in receptor recognition.

Conclusions

In this paper we have studied a fully potent analogue of insulin containing mutations that selectively destabilize both the dimer contact (ProB28 → Lys; LysB29 → Pro) and the hexamer contact (HisB10 → Asp). This analogue (designated DKP-insulin) provides a model of the insulin monomer, which is the physiologically active form of the hormone. 2D NMR spectra of DKP-insulin, unlike that of the native protein, are well resolved in pH range 6–8 and demonstrate extensive tertiary structure. ^{13}C and ^{2}H NMR labels, introduced at positions B23–B26 by trypsin-mediated semisynthesis, provide intrinsic probes for the structure of the hydrophobic core and the dynamics of the receptor-binding surface. These studies confirm and extend under physiological conditions the results of a previous 2D NMR analysis of native insulin in 20% acetic acid (Hua & Weiss, 1991).

Comparison of observed and predicted NMR features leads to the following conclusions. (i) Mutations at positions B28-B29 and B10 contribute independently to the structure and function of insulin, suggesting that the dimer- and hexamer-related surfaces may be regarded as independent design features. (ii) Stabilizing interactions are observed involving IleA2, TyrA19, ValB12, LeuB15, and PheB24. The hydrophobic core is in general similar to that observed in crystal structures and previously described in the solution structure of des-pentapeptide insulin (DPI) in 20% acetic acid (Hua & Weiss, 1990). (iii) The side chain of TyrB26, a probe for the C-terminal region of the B-chain, is well-ordered. NOEs to ValB12, LeuB15, and IleA2 indicate that it packs against the hydrophobic core in accord with crystal models. (iv) The side chain of ArgB22 (but not that of Lys B28) exhibits inequivalent distal proton resonances and so is likely to participate in a salt bridge(s) on the surface of the protein in accord with crystal models. (v) Global flexibility is suggested by several observations, including the overall attenuation (quenching) of nonlocal NOEs relative to the predictions of crystal models, the rapid exchange of amide protons with solvent, and the absence of significant barriers to the rotation of internal aromatic rings ("ring flips") on the ^{1}H and ^{13}C time scales. Differential broadening of amide resonances is also observed; such broadening has previously been attributed to millisecond motions in the protein, i.e., conformational exchange involving relative displacement of elements of secondary structure (Weiss et al., 1989). (vi) Local flexibility in the putative receptor-binding surface is indicated by the absence of predicted tertiary NOEs involving B23 and B25. The side chain of PheB25 adopts primarily an outward configuration and is thus positioned to interact directly with the insulin receptor.

The present results establish elements of structure and flexibility in an engineered insulin monomer and provide a base line for further studies of mutations associated with enhanced or diminished affinity for the insulin receptor. By correlating structure and function, such studies may in the future establish design rules for the engineering of novel insulins in diabetes management.

Acknowledgments

NMR spectra were obtained at Harvard Medical School (NIH 1 S10 RR04862-01), the University of Wisconsin NMR Facility (NIH RR-02301 and NSF PCM-8415048), and the MIT National Magnet Laboratory (NIH RR-00995). We thank R. E. Chance and R. DiMarchi (Eli Lilly & Co.) for insulin analogues and advice; M. Chaudhuri for synthesis of labeled peptides; J. Lee, M. Kochoyan (Harvard Medical School), A. Bax (NIH), and W. M. Westler (University of Wisconsin, Madison) for helpful discussion concerning NMR techniques; D. Nguyen and M. Karplus for communication of results prior to publication; M. Nilges and A. T. Brunger for XPLOR and helpful discussion; V. Hruby (University of Arizona) for generously providing ^{13}C-labeled tyrosine used in pilot experiments; C. R. Kahn, G. G. Dodson, T. E. Blundell, O. M. Rosen, M. Dunn, G. Wagner, and J. Avruch for encouragement and helpful discussion; and L. J. Neuringer (MIT Magnet Laboratory) for support in the early stages of the work. Q.-X.H. was supported in part by an NIH resource grant to the MIT Francis Bitter National Magnet Laboratory (RR-0995). M.A.W. and S.E.S. thank Prof. Christopher T. Walsh, Eugene Braunwald, and John T. Potts, Jr. for their encouragement.

Supplementary Material Available

Three figures showing the 1D ^{1}H NMR spectrum of DKP-insulin in H_2O solution (pH 6.5), the 1D isotope-edited spectrum of the GlyB23-H_α resonances, and TOCSY spectra

of selectively deuterated DKP–insulin analogues (residues B24, B25, and B26) and one table giving ring-current shift calculations for methyl-containing residues (8 pages). Ordering information is given on any current masthead page.

References

Adams, M. J., Blundell, T. E., Dodson, E. J., Dodson, G. G., Viyayan, M., Baker, E. N., Hardine, M. M., Hodgkin, D. C., Rimer, B., & Sheet, S. (1969) *Nature (London) 224*, 491–495.

Baker, E. N., Blundell, T. E., Cutfield, G. S., Cutfield, S. M., Dodson, E. J., Dodson, G. G., Hodgkin, D. M. C., Hubbard, R. E., Iassac, M. W., Reynolds, D. C., Sakabe, K. S., Sakabe, N., & Vjayan, N. M. (1988) *Philos. Trans. R. Soc. London, B 319*, 389–456.

Bentley, G. A., Dodson, E. J., Dodson, G. G., & Levitova, A. (1978) *J. Mol. Biol. 125*, 387–396.

Bi, R. C., Dauter, Z., Dodson, E., Dodson, G., Giordano, F., & Reynolds, C. (1984) *Biopolymers 23*, 391–395.

Blundell, T. E., & Humbel, R. E. (1980) *Nature (London) 287*, 781–787.

Blundell, T. E., Cutfield, J. F., Cutfield, S. M., Dodson, E. J., Dondson, G. G., Hodgkin, D. C., Mercola, D. A., & Vijayan, M. (1971) *Nature (London) 231*, 506–511.

Boelens, R., Ganadu, M. L., Verheyden, P., & Kaptein, R. (1990) *Eur. J. Biochem. 191*, 147–153.

Bradbury, J. H., & Wilairiat, P. (1967) *Biochem. Biophys. Res. Commun. 29*, 84–89.

Bradbury, J. H., & Brown, L. R. (1977) *Biochemistry 16*, 573–582.

Bradbury, J. H., Ramesh, R., & Dodson, G. (1981) *J. Mol. Biol. 150*, 609–613.

Bradbury, J. H., & Ramesh, V. (1985) *Biochem. J. 229*, 731–737.

Brange, J., Ribel, U., Hansen, J. F., Dodson, G., Hansen, M. T., Havelund, S., Melberg, S. G., Norris, F., Norris, K., Snel, L., Sorensen, A. R., & Voigt, H. O. (1988) *Nature 333*, 679–682.

Brange, J., Owens, D. R., Kang, S., & Volund, A. (1990) *Diabetes Care 13*, 923–954.

Bromer, W. W., & Chance, R. E. (1967) *Biochim. Biophys. Acta 133*, 219–223.

Brooks, B. R., Bruccoler, R. E., Olafson, B. O., States, D. J., Swaminathan, S., & Karplus, M. (1983) *J. Comput. Chem. 4*, 187–217.

Carroll, R. J., Hammer, R. E., Chan, S. J., Shift, H. H., Rubenstein, A. H., & Steiner, D. F. (1988) *Proc. Natl. Acad. Sci. U.S.A. 85*, 8943–8947.

Chan, S. J., Seino, S., Grapppuso, P. A., Gordan, P., & Steiner, D. F. (1987) *Proc. Natl. Acad. Sci. U.S.A. 84*, 2194–2197.

Cheshnovsky, D., Neuringer, L. J., & Williamson, K. L. (1983) *J. Protein Chem. 1*, 335–339.

Chothia, C., Lesk, A. M., Dodson, G. G., & Hodgkin, D. C. (1983) *Nature (London) 302*, 500–505.

Davis, D. G., & Bax, A. (1985) *J. Magn. Reson. 64*, 533–535.

Dayhoff, M. O., Ed. (1972) *Atlas of Protein Sequence and Structure*, Vol. 5, Biomedical Research Foundation, Bethesda, MD.

Derewenda, U., Derewenda, Z., Dodson, E. J., Dodson, G. G., Reynolds, C. D., Smith, G. D., Sparks, C., & Swenson, D. (1989) *Nature (London) 338*, 594–596.

Dodson, E. J., Dodson, G. G., & Hodgkin, D. C. (1979) *Can. J. Biochem. 57*, 469–479.

Dodson, E. J., Dodson, G. G., Hubbard, R. E., & Reynolds, C. D. (1984) *Biopolymers 22*, 281–291.

Ebina, Y., Edery, M., Ellis L., Standing, D., Beaudoin, J., Roth, R. A., & Rutter, W. J. (1985) *Proc. Natl. Acad. Sci. U.S.A. 82*, 8014–8018.

Fischer, W. H., Saunders, D., Brandenburg, D., Wollmer, A., & Zahn, H. (1985) *Biol. Chem. Hoppe-Seyler 366*, 521–525.

Fischer, W. H., Saunders, D., Diaconescu, C., Brandenburg, D., Wollmer, A., Dodson, G., De Meyts, P., & Zahn, H. (1986) *Biol. Chem. Hoppe-Seyler 367*, 999–1006.

Goldman, J., & Carpenter, F. H. (1974) *Biochemistry 13*, 4566–4574.

Gross, D. J., et al. (1989) *Proc. Natl. Acad. Sci. U.S.A. 86*, 4107–4111.

Gruppuso, P. A., Gorden, P., Kahn, C. R., Cornblath, M., Zeller, W. P., & Schwartz, R. (1984) *N. Engl. J. Med. 311*, 629–643.

Haneda, M., Polonsky, K. S., Bergenstal, R. M., Jaspan, J. B., Shoelson, S. E., Blix, P. M., Chan, S. J., Kwok, S. C. M., Wishner, W. B., Zeidler, A., Olefsky, J. M., Freidenberg, G., Tager, H. S., Steiner, D. F., & Rubenstein, A. H. (1984) *N. Engl. J. Med 310*, 1288–1294.

Hoch, J. C., Dobson, C. M., & Karplus, M. (1982) *Biochemistry 21*, 132–140.

Hua, Q.-X., Chen, Y.-J., Wang, C.-C., Wang, D.-C., & Roberts, G. C. K. (1989) *Biochim. Biophys. Acta 994*, 114–120.

Hua, Q. X., & Weiss, M. A. (1990) *Biochemistry 29*, 10545–10555.

Hua, Q. X., & Weiss, M. A. (1991) *Biochemistry 30*, 5505–5515.

Inouye, K., Watanabe, K., Morihara, K., Tochino, Y., Kanaya, T., Emura, J., & Sakakibara, S. (1979) *J. Am. Chem. Soc. 101*, 751–752.

Inouye, K., Watanabe, K., Tochino, Y., Kobayashi, M., & Shigeta, Y. (1981a) *Biopolymers 20*, 1845–1858.

Inouye, K., Watanabe, K., Tochino, Y., Kanaya, T., Kobayashi, M., & Shigeta, Y. (1981b) *Experientia 37*, 811–813.

Inouye, K., Watanabe, K., Tochino, Y., Kobayashi, M., & Shigeta, Y. (1983) in *Peptide Chemistry 1982* (Sakakibara, S., Ed.) pp 277–282, Protein Research Foundation, Osaka, Japan.

Jeffrey, P. D., & Coates, J. H. (1966a) *Biochemistry 5*, 489–498.

Jeffrey, P. D., & Coates, J. H. (1966b) *Biochemistry 5*, 3820–3825.

Jeffrey, P. D., Milthorpe, B. K., & Nichol, L. W. (1976) *Biochemistry 15*, 4660–4665.

Johnson, C. E., & Bovey, F. A. (1958) *J. Chem. Phys. 29*, 1012–1017.

Kang, S., Owens, D. R., Vora, J. P., & Brange, J. (1990) *Lancet 335*, 303–306.

Kaptein, R. (1980) in *Photo-CIDNP Studies of Proteins in Biological Magnetic Resonance* (Berliner, W., & Rueben, J., Eds) Vol. 4, pp 145–191, Plenum Press, New York, NY.

Kline, A. D., & Justice, R. M., Jr. (1990) *Biochemistry 29*, 2906–2913.

Kobayashi, M., Ohgaku, S., Iwasaki, M., Maegawa, H., Shigeta, Y., & Inouye, K. (1982a) *Biochem. J. 206*, 597–603.

Kobayashi, M., Ohgaku, S., Iwasaki, M., Maegawa, H., Shigeta, Y., & Inouye, K. (1982b) *Biochem. Biophys. Res. Commun. 107*, 329–336.

Kowalsky, A. (1962) *J. Biol. Chem. 237*, 1807–1819.

Kristensen, S. M., Jorgensen, A. M. M., & Led, J. J. (1991) *J. Mol. Biol. 218*, 221–231.
Kruger, P., Strassburger, W., Wollmer, A., van Gunsteren, W. F., & Dodson, G. G. (1987) *Eur. Biophys. J. 14*, 449–459.
Kubiak, T., & Cowburn, D. (1986) *Int. J. Pept. Protein Res. 27*, 514–521.
Mirmira, R., & Tager, H. S. (1989) *J. Biol. Chem.* 264, 6349–6354.
Muszkat, K. A., Khait, I., & Weinstein, S. (1984) *Biochemistry 23*, 5–10.
Nakagawa, S. H., & Tager, H. S. (1986) *J. Biol. Chem. 261*, 7332–7341.
Nakagawa, S. H., & Tager, H. S. (1987) *J. Biol. Chem. 262*, 12040–12058.
Paselk, R. A., & Levy, D. (1974) *Biochim. Biophys. Acta 359*, 215–221.
Pekar, A. H., & Frank, B. (1972) *Biochemistry 11*, 4013–4016.
Peking Insulin Structure Group (1971) *Peking Rev. 40*, 11–16.
Perkins, S. J., & Dwek, R. A. (1980) *Biochemistry 19*, 245–253.
Pullen, R. A., Lindsay, D. G., Wood, S. P., Tickle, I. J., Blundell, T. L., Wollmer, A., Krail, A., Brandenburg, D., Zahn, H., Gliemann, J., & Gammeltoft, S. (1976) *Nature (London) 259*, 369–373.
Roy, M., Lee, R. W.-K., Brange, J., & Dunn, M. F. (1990) *J. Biol. Chem. 265*, 5448–5453.
Schwartz, G. P., Burke, G. T., & Katsoyannis, P. G. (1987) *Proc. Natl. Acad. Sci. U.S.A. 84*, 6408–6411.
Schwartz, G. P., Burke, G. T., & Katsoyannis, P. G. (1989) *Proc. Natl. Acad. Sci. U.S.A. 86*, 458–461.
Shoelson, S. E., Haneda, M., Blix, P., Nanjo, K., Sanke, T., Inouye, K., Steiner, D., Rubenstein, A., & Tager, H. (1983a) *Nature (London) 302*, 540–542.
Shoelson, S. E., Fickova, M., Haneda, M., Nahum, A., Musso, G., Kaiser, E. T., Rubenstein, A. H., & Tager, H. (1983b) *Proc. Natl. Acad. Sci. U.S.A. 80*, 7390–7394.
Shoelson, S. E., Lu, Z.-X., Parlavtan, L., Lynch, C. S., & Weiss, M. A. (1991) *J. Biol. Chem.* (submitted for publication).
Sklenar, V., & Bax, A. (1987) *J. Magn. Reson. 75*, 378–383.
Smith. G. D., Swenson, D. C., Dodson, G. G., & Reynolds, C. D. (1984) *Proc. Natl. Acad. Sci. U.S.A. 81*, 7093–7097.
States, D. J., Haberkorn, R. A., & Ruben, D. J. (1982) *J. Magn. Reson. 48*, 286–292.
Steiner, D. F., Bell, G. I., & Tager, H. S. (1989) in *Endocrinology* (DeGroot, L. J., Ed.), pp 1263–1289, Grune & Stratton, New York.
Strickland, E. H., & Mercola, D. A. (1976) *Biochemistry 15*, 3875–3884.
Stewart, J. M., & Young, J. D. (1984) *Solid Phase Peptide Synthesis*, Raven Press, New York.
Tager, H., Given, B., Baldwin, D., Mako, M., Markese, J., Rubenstein, A., Olefsky, J., Kobayashi, M., Kolterman, O., & Poucher, R. (1979) *Nature (London) 281*, 122–125.
Tager, H., Thamoas, N., Assoian, R., Rubenstein, A., Saekow, M., Olefsky, J., & Kaiser, E. T. (1980) *Proc. Natl. Acad. Sci. U.S.A. 77*, 3118–3185.
Torda, A. E., Sheek, R. M., & van Gunsteren, W. F. (1990) *J. Mol. Biol. 14*, 223–235.
Wagner, G., & Wuthrich, K. (1982) *J. Mol. Biol. 155*, 347–366.
Weiss, M. A., & Hoch, J. C. (1987) *J. Magn. Reson. 72*, 324–333.
Weiss, M. A., Nguyen, D. T., Khait, I., Inouye, K., Frank, B. H., Beckage, M., O'Shea, E. K., Shoelson, S. E., Karplus, M., & Neuringer, L. J. (1989) *Biochemistry 28*, 9855–9873.
Weiss, M. A., Frank, B. H., Khait, I., Pekar, A., Heiney, R., Shoelson, S. E., & Neuringer, L. J. (1990) *Biochemistry 29*, 8389–8401.
Williamson, K. L., & Williams, R. J. P. (1979) *Biochemistry 18*, 5966–5972.
Wollmer, A., Fleischhauer, J., Strassburger, W., Thiele, H., Bradenburg, D., Dodson, G., & Mercola, D. (1979) *Biophys. J. 20*, 233–243.
Wollmer, A., Strassburger, W., Glatter, U., Dodson, G. G., & McRittel, W. (1981) *Hoppe-Seyler's Z. Physiol. Chem. 362*, 581–591.
Wood, S. P., Blundell, T. L., Wollmer, A., Lazarus, N. R., & Neville, R. W. J. (1975) *Eur. J. Biochem. 55*, 531–542.
Wuthrich, K. (1986) *NMR of Proteins and Nucleic Acids*. John Wiley & Sons, New York, NY.
Wuthrich, K. (1989) *Methods Enzymol.*
Wuthrich, K., Wider, G., Wagner, G., & Braun, W. (1983) *J. Magn. Reson. 155*, 311.
Yajima, H., Fujii, N., Funakoshi, S., Watanabe, T., Murayama, E., & Otaka, A. (1988) *Tetrahedron 44*, 805–819.